

## Sediment Organic Matter in Areas of Intense Methane Release in the Laptev Sea: Characteristics of Molecular Composition

A.A. Grinko<sup>a,✉</sup>, I.V. Goncharov<sup>a,b</sup>, N.E. Shakhova<sup>a</sup>, Ö. Gustafsson<sup>c</sup>, N.V. Oblasov<sup>b</sup>, E.A. Romankevich<sup>d</sup>, A. G. Zarubin<sup>a</sup>, R.S. Kashapov<sup>b</sup>, D.V. Chernykh<sup>c</sup>, E.V. Gershelis<sup>a</sup>, O.V. Dudarev<sup>a,e</sup>, A.K. Mazurov<sup>a</sup>, I.P. Semiletov<sup>a,e</sup>

<sup>a</sup> National Research Tomsk Polytechnic University, pr. Lenina 30, Tomsk, 634050, Russia

<sup>b</sup> JSC «TomskNIPIneft», pr. Mira 72, Tomsk, 634027, Russia

<sup>c</sup> Stockholm University, Department of Environmental Science and Analytical Chemistry Bolin Centre for Climate Research, Stockholm, Sweden

<sup>d</sup> P.P. Shirshov Institute of Oceanology of the Russian Academy of Sciences, Nakhimovskii pr. 36, Moscow, 117997, Russia

<sup>e</sup> V.I. Il'ichev Pacific Oceanological Institute, Far Eastern Branch of the Russian Academy of Sciences, ul. Baltiyskaya 43, Vladivostok, 690041, Russia

Received 10 May 2018; received in revised form 19 April 2019; accepted 22 May 2019

**Abstract**—We present results of study of the molecular composition of organic matter (OM) in the bottom sediments of the Laptev Sea by gas chromatography–mass spectrometry, isotope gas chromatography–mass spectrometry, and Rock-Eval pyrolytic analysis. The OM of all collected sediment samples shows a significant terrigenous contribution. Compounds that are biomarkers of methanotrophic microorganisms are also found. A positive correlation between the contents of the studied biomarkers and the contents of pelite and total organic carbon is observed at the sites with documented intense methane bubbling. For example, the average content of C30 hopenes at the “methane” stations is twice higher than that at the “background” ones. The average content of C32  $\alpha\beta$ -hopanes in sediment samples from the methane seepage area is 1.5 times higher than that at the background stations. We suggest that the increased C30  $\alpha\beta$ -hopane content (~1.5 times higher within the methane seepage area) and the decreased moretane index relative to the C31 hopane index are due to the inflow of OM of petroleum origin. The presence of biphenyl in sediments indicates its petroleum origin, which supports our assumption of the migratory nature of petroleum hydrocarbons in the methane seepage area. Triterpenoids found in the sediment OM indicate diagenetic bacterial transformation of OM in the methane seepage areas, which shows that methane has been released for a long time. We assume the intense activity of the consortium of methanotrophs and sulfate reducers in the methane seepage areas.

**Keywords:** methane emissions; organic matter; bottom sediments; hopanoids; methanotrophs; Arctic; Laptev Sea

### INTRODUCTION

The Siberian Arctic shelf makes up half the shelf of the entire Arctic Ocean and contains huge reserves of hydrocarbon resources (Gramberg et al., 1983; Kontorovich et al., 2013). This work focuses on the East Siberian Shelf (ESS), since it is on the ESS that there are prerequisites for the development of the most serious consequences associated with current climate change (Shakhova and Semiletov, 2009). The ESS is the largest and shallow shelf of the World Ocean, its entire area is covered by submarine permafrost, which has degraded at double speed for the last 30 years (Shakho-

va et al., 2017). In addition, a large amount of material of terrigenous origin arrives at the ESS, which integrates changes occurring in the hydrological and biogeochemical cycles of terrestrial ecosystems in response to climate change and degradation of the land permafrost (Semiletov et al., 2000; Gustafsson et al., 2011; Vonk et al., 2012, 2014; Pugach et al., 2017; 2011, 2012, 2013). This area is warming faster than any other with the Arctic region (Luchin et al., 2002; Proshutinsky et al., 2012; Stroh et al., 2015). Moreover, this unique shelf contains more than 80% of the world's subsea permafrost, and also contains the main proportion of the shallow shelf gas hydrates, whose stability depends on the thermal state of the subsea permafrost (Romanovskii et al., 2005; Shakhova and Semiletov, 2009; Shakhova et al., 2009a,b; Nicolisky and Shakhova, 2010;

✉ Corresponding author.

E-mail address: grinko@tpu.ru (A.A. Grinko)

Shakhova et al., 2010a,b, 2014, 2015, 2017; Nicolsky et al., 2012). Nowadays thermal state of the subsea permafrost approach to the melting point and in some areas it has already reached it, which has led to the mobilization and involvement of huge amounts of ancient organic carbon (OC) in the modern biogeochemical cycle and an increase in the emission of major greenhouse gases ( $\text{CO}_2$  and  $\text{CH}_4$ ) into the atmosphere region (Semiletov et al., 2007, 2012; Shakhova et al., 2010a,b,c, 2014, 2015; Anderson et al., 2011; Pipko et al., 2011, 2017; Sergienko et al., 2012). There is a huge amount of OC in the thick sediments of the ESS (they reach 15–20 km), which is many orders of magnitude greater than the OC reserves on land (Romankevich and Vetrov, 2001; Vetrov and Romankevich, 2004; Macdonald et al., 2008), which can be included in the modern biogeochemical cycle (seasonally thawed layer), due to the degradation of the upper layer of permafrost. Therefore, the involvement of even a small fraction of the OC buried in the permafrost into the biogeochemical cycle can lead to unpredictable environmental and climatic consequences (Semiletov, 1999; Shakhova et al., 2009a,b, 2010; Shakhova and Semiletov, 2009; Semiletov et al., 1996, 2004; Vonk et al., 2012, 2014). In the number of recent studies it was shown that the oxidation of erosional OC is the main source of  $\text{CO}_2$  and acidification of ESS waters (Semiletov et al., 2016), and the main source of  $\text{CH}_4$  is its discharge from bottom sediments into the water column and atmosphere, due to the degradation of subsea permafrost (Shakhova et al., 2010a,b, 2014, 2015, 2017; Leifer et al., 2017). As the most realistic candidate for explaining massive  $\text{CH}_4$  bubble emissions from bottom sediments (up to hundreds of grams per square meter per day (Shakhova et al., 2015; Leifer et al., 2017)) into the water column and atmosphere is considered destabilization of gas hydrates, the state of which is controlled by the state of the subsea permafrost (Shakhova et al., 2010a,b, 2015, 2017). First studies of methane isotopic composition (Sapart et al., 2017) were performed for understanding of the nature of bubble  $\text{CH}_4$ , but these studies were not enough for an unambiguous interpretation of methane bubble origin. Obviously, the solution of such a fundamental problem requires comprehensive investigations aimed at studying the qualitative and quantitative composition of the OC of the bottom sediments, the degree of their biogeochemical transformation within and beyond the areas of intense emissions.

The purpose of this work is to study and determine the characteristic features of the organic matter composition of the Laptev Sea bottom sediments within and beyond the areas of intense emissions. In this work recent bottom sediments in the most studied part of the ESS (the Laptev Sea) are considered as accumulators of signals indicating various processes, which lead to transformation of the OC composition and characterize sedimentation conditions (van Dongen et al., 2008; Cooke et al., 2009; Semiletov et al., 2012; Tesi et al., 2014; Vonk et al., 2014; Selver et al. 2015; Xiao et al., 2015; Bröder et al., 2016; Dudarev et al., 2016; Panova et al., 2017; Semiletov et al., 2017). It is assumed that the use

of different types of biomarkers will contribute to understanding geochemical processes, which, within the study area, are connected with the emission of  $\text{CH}_4$  from bottom sediments into the water column and atmosphere, this is crucial to identify the main sources of  $\text{CH}_4$ , their qualitative and quantitative assessment.

## STUDY AREA

The Laptev Sea with an area of  $500 \cdot 10^3 \text{ km}^2$  with an average water depth of about 50 m (Jakobsson et al., 2008), accepts dissolved and suspended terrigenous OC from the vast drainage area of the largest rivers of Eastern Siberia — the Lena, the Yana, and the Khatanga (Dobrovolsky and Zalogin, 1982; Gustafsson et al., 2011; Semiletov et al., 2011, 2012). In recent years, it has been established that the main source of suspended OC on the Laptev Sea shelf is erosion of the coast ice complex deposits (Grigoriev et al., 2004; Karlsson et al., 2011; Semiletov et al., 2011, 2013; Vonk et al., 2012, 2014), but not river runoff, as it was considered before. However, suspended soil OC can appear in large quantities in the anomalous years (Charkin et al., 2011) and geological epochs (Tesi et al., 2016), as well as during high freshet from the drainage basin of the Lena River (3 million sq. km), which may lead to the most extremely  $^{13}\text{C}$  depleted OC in the surface sediments northwest of the New Siberian Islands (Sánchez-García et al., 2011).

Climate warming is most pronounced in the Arctic, as evidenced by a significant increase in air temperature, an increase in river flow, and a decrease in ice cover [Semiletov et al., 2000; Luchin et al., 2002; Report..., 2007]. Based on many years of observations [<http://rims.unh.edu/>], it is shown that the annual flow of the Lena River in the period 1999–2008 varied between  $457 \text{ km}^3$  and  $716 \text{ km}^3$ , and the average annual flow for this period ( $583 \text{ km}^3$ ) is about 11% higher than the average annual flow for the previous decade (1990–1999) (Semiletov et al., 2013), which resulted in a significant warming of the Laptev Sea coastal waters (Shakhova et al., 2014).

The Laptev Sea is characterized by low annual average water temperatures varying from  $-1.8 \text{ }^\circ\text{C}$  in the north to  $-0.8 \text{ }^\circ\text{C}$  in the southeastern part (Dobrovolsky and Zalogin, 1982), which is explained by the warming effect of river flow and effective mixing of waters till to the bottom (Shakhova et al., 2014), this manifests itself in positive summer temperatures of bottom water and surface bottom sediments, including the Dmitry Laptev Strait in the East Siberian Sea (Shakhova and Semiletov, 2009). Diffusion of heat and convective salinization of bottom sediments of the coastal zone, which is characterized by the predominance of the psammitic fraction, leads to high rates of subsea permafrost degradation and the formation of deep (open) taliks (Shakhova et al., 2017).

From the north, it is bounded by the Eurasian Ocean Basin, which accommodates the axial Gakkel Ridge, the ex-

treme link in the world system of spreading ridges, which ends at the Laptev Sea continental slope (Imaev et al., 1990; Drachev, 2000). Thus, it is one of few places, where active spreading axis is adjacent to the edge of the continent, which has overriding importance for studying the split of the continents and the origin of the oceans (Franke et al., 2001). The ambiguity and inconsistency of ideas about the geological structure of the Laptev Sea Plate are due to extremely complex fault tectonics (Leonov et al., 2007; Andieva, 2008). The Laptev Sea represents a unique articulation of the active spreading axis (Gakkel ridge) and the continental margin, important for studying the fault of the continents. The modern understanding of the tectonics of this region is based on the results of marine multichannel seismic profiling, the latest gravimetric data and geological studies of the continental framing. The structure of the shelf is represented by a series of deep rifts and high standing foundation blocks forming the rift system. From the west to the east, the South Laptev Sea Rift Basin, the Ust-Lena Rift, the East Laptev Sea and Stolbovko horsts, the Bel'kov-Svyatoy Nos and Anisinsky Rifts are distinguished (Fig. 1b) (Drachev, 2000). Sedimentary filling of rifts is underlain by a heterogeneous folded basement of Mesozoic consolidation (Andieva, 2008).

Due to the absence of deep drilling, the material composition of the complexes of the Laptev Sea sedimentary section can only be determined approximately on the basis of the characteristics of seismic recording and their comparison with the data on framing and transgressive regressive events in the Arctic (Leonov et al., 2007). It can be assumed that the characteristic features of the disjunctive tectonics studied in detail and certified by deep core drilling in the Anabar–Lena zone, which adjacent to the Laptev Sea (Kontorovich et al., 2013), are similar to those of the Laptev Sea. If this assumption is valid, we can propose that on the Laptev Sea Shelf, by analogy with the northern part of the Anabar–Lena zone, there are faults that cut through the entire sedimentary cover and penetrate into the Mesozoic. It is possible that these faults penetrate deeper, which to some extent may testify in favor of the hypothesis about a deep source of methane with an anomalously young radiocarbon age (Sapart et al., 2017) whose massive discharge was documented in the northern part of the Laptev Sea (Shakhova et al., 2015; Leifer et al., 2017). The density modeling data confirm that the sedimentary cover on the Laptev Sea Shelf lies on the Mesozoic folded basement (Andieva, 2008).

The change in water salinity is determined by the river runoff and sea ice melting, as well as hydrometeorological factors. Salinity values change in winter from 20–25‰ in the southeast to 34‰ in the northern areas of the sea, and in summer, due to the increasing freshwater flow, the salinity decreases to 5–10‰ and 30–32‰ respectively (Dobrovolsky and Zalogin, 1982; Dudarev, 2016; Pipko et al., 2017). In work (Semiletov et al., 2016), it was shown that the distribution area of surface waters desalinated by the Lena River, marked with isochaline 23, increased by 116 thou-

sand km<sup>2</sup> over the period (2000–2012) compared with the period (1932–2000), which indicates a steady long-term trend of warming and growth of the Lena River flow, which was first shown for the second half of the 20th century in works (Savelieva et al., 2000; Semiletov et al., 2000).

It follows from the above that the Laptev Sea is one of the areas most affected by climate warming and the corresponding changes in the land – cryosphere – sea system.

The study area in this paper is a polygon located in the northern part of the Laptev Sea (Fig. 1) between 76.5–77.5°N and 121–132°E, with total area approximately 6400 km<sup>2</sup>, and denoted as P1 (Shakhova et al., 2015). This site represents the outer shelf, where melting of permafrost was predicted, and intense methane bubbling associated with destabilization of subsea permafrost were detected (Shakhova et al., 2015, 2017).

The content of organic matter in the investigated polygon is characterized as relatively high for the Arctic region (more than 0.5% on average) (Tissot and Welte, 1984; Fahl and Stein, 1997; Vetrov and Romankevich, 2004). The most complete map of the OC distribution in the surface sediments of the Laptev Sea and the East Siberian Sea is given in (Shakhova et al., 2015), and for the investigated polygon it is shown in Fig. S10.<sup>1</sup>

## MATERIALS AND METHODS

**Sampling.** Samples of recent bottom sediments studied in the course of the research (Table 1) were collected by the staff of the Arctic Research Laboratory of the V.I. Il'ichev Pacific Oceanological Institute in the northern part of the Laptev Sea in the framework of the marine research expedition in 2011 (R/V Akademik Lavrent'ev) (Sergienko et al., 2012). The Van Veen grab sampler and the direct-flow gravity tube were used as the technical devices for sampling. The sampling interval for all samples was 0–5 cm. Samples were stored in a frozen state. The P1 investigated polygon, where samples were collected during the expedition, is shown in Fig. 1 in the upper left corner.

The collected samples in the course of the research were stored in the laboratory in a frozen state.

**Sample preparation.** Samples were thawed at the room temperature for 24 hours and then homogenized. Next, the samples were brought to constant weight in a desiccator at the temperature of 45 °C. Extraction of the bottom sediments samples (separation of the bitumoid) was performed with chloroform in the Soxhlet apparatus for at least 14 h. Then the extracts were concentrated on a rotary evaporator and dried to constant weight in the desiccator.

**Rock-Eval pyrolytic analysis.** The total content of organic carbon, the content of mineral carbon, the content of volatile organic compounds (peak S1, see Fig. S1), the amount of the destruction products of protokerogen (peak

<sup>1</sup> [http://sibran.ru/journals/Supplementary\\_tables\\_figures.pdf](http://sibran.ru/journals/Supplementary_tables_figures.pdf)

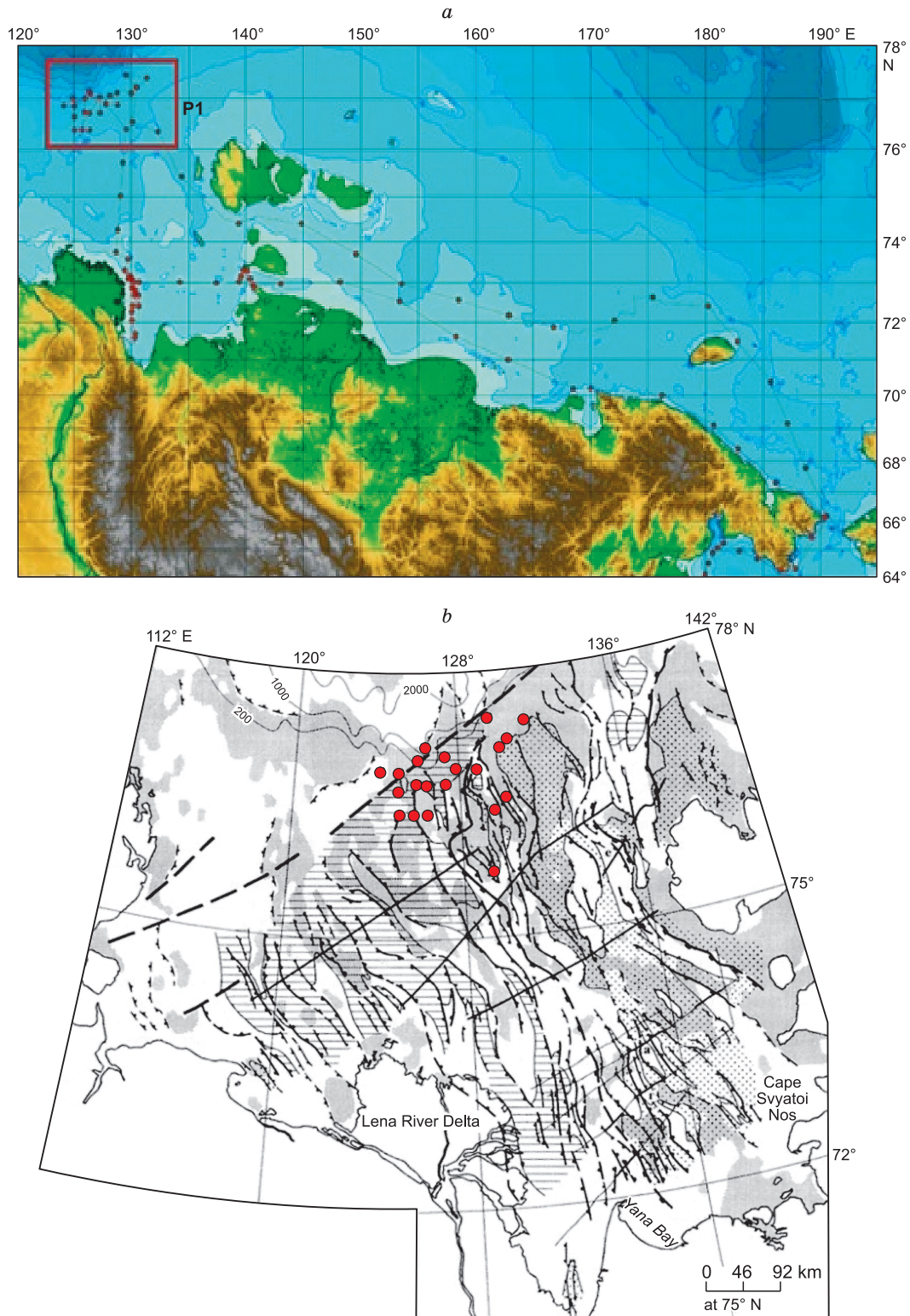


**Fig. 1.** The study area (the investigation polygon in the upper left corner, enclosed with a red line,) polygon P1 (a) (Shakhova et al., 2015), and the stations of the test site (the study area is marked with a rectangle), plotted on the map with the structural scheme of the Laptev Sea rift system (b) (Drachev, 2000).

**Table 1.** Stations coordinates, depth of sampling, and degree of diagenetic transformation of sediments.<sup>1</sup>

№ st.	Coordinates of the stations, °				Depth, m		IDM	Pr/C <sub>17</sub>	Phy/C <sub>18</sub>	T <sub>max</sub> , °C
	Start		End		Echosounder	CTD				
	Latitude	Longitude	Latitude	Longitude						
20	76.554	130.136	76.556	130.133	60.0	60	0.44	0.29	0.30	339
21	77.210	130.471	77.212	130.477	65.6	67	0.42	0.34	0.37	341
22	77.440	129.550	77.442	129.555	85.0	86	0.36	0.26	0.22	344
23	77.383	131.398	77.386	131.402	67.0	68	0.42	0.25	0.19	335
25	77.101	130.007	77.103	130.013	60.0	60	0.44	0.27	0.22	340
28	77.000	125.985	76.997	125.990	91.3	92	0.38	0.24	0.16	344
29	76.736	125.905	76.732	125.910	67.3	68	0.43	0.23	0.21	341
30	76.392	125.755	76.388	125.754	50.0	50	0.43	0.25	0.14	335
32	77.029	127.289	77.029	127.289	74.0	74	0.42	0.14	0.21	336
33	76.721	127.309	76.720	127.313	65.0	66	0.45	0.28	0.16	332
34	76.720	126.396	76.720	126.401	66.0	67	0.41	0.18	0.14	338
35	76.392	126.423	76.393	126.431	49.0	49	0.41	0.55	0.32	340
36	76.398	125.051	76.397	125.057	62.0	62	0.42	0.43	0.18	347
37	76.648	125.048	76.648	125.055	70.0	69	0.42	0.42	0.26	334
38	76.859	125.047	76.856	125.047	86.0	86	0.40	0.41	0.30	343
40	76.867	124.134	76.863	124.135	103.0	103	0.42	0.47	0.24	344
43	77.143	126.368	77.140	126.366	651.0	651	0.34	0.34	0.26	362
44	76.896	127.812	76.895	127.806	64.0	64	0.38	0.48	0.17	337
45	76.880	128.834	76.876	128.827	69.0	69	0.41	0.38	0.26	336
48	76.410	129.573	76.410	129.573	57.0	57	0.39	0.38	0.20	339
49	75.734	129.301	75.733	129.306	46.0	46	0.39	0.39	0.36	361

Note. <sup>1</sup>The degree of diagenetic transformation of sediments is determined by the coefficients Pr/C<sub>17</sub>, Phy/C<sub>18</sub>, defined using the GC-MS method (Pr, pristane, Phy, phytane) and by pyrolytic method Rock-Eval (IDM index). IDM, index of diagenetic maturity determined by Rock-Eval analysis. IDM is equal to the ratio of the number of pyrolytic hydrocarbons released under temperature up to 380 °C to the total amount of hydrocarbons (Menevsky et al., 2017).

CTD, oceanographic probe for depth measurement.

T<sub>max</sub>, temperature of the maximum rate of hydrocarbon generation during Rock-Eval pyrolysis.

S2, see Fig. S1) in the sediments were determined on a “Rock-Eval 6 Turbo” pyrolyzer produced by VINCI Technologies. Temperature program was as follows: start heating the sample was 300 °C, holding for 3 minutes, then heating to 650 °C with the heating rate of 25 °C/min.

**GC-MS analysis of the extracts.** The obtained extracts were investigated by gas chromatography-mass spectrometry (GC-MS) method on the Bruker SCION 436 GC TQ instrument using the HP-5MS quartz capillary column (length 30 m, internal diameter 0.25 mm, film thickness 0.25 μm). Analysis conditions were as follows: inlet temperature was 300 °C, initial oven temperature was 40 °C, followed by heating with the rate 5 °C/min to 150 °C, then 3 °C/min to 310 °C, and holding at 310 °C 20 min. The velocity of the carrier gas (helium) was 1.1 ml/min, the volume of the injected sample was 1 μl (the solvent is hexane). Measurements were carried out both on the total ion current, and on the selected ions (in the Scan and SIM modes), as well as in the MS-MS mode on GC-MS Agilent 7890B (GC)–Agilent Q-TOF 7200 (MS) instrument with the same temperature program (quartz capillary column HP-1MS, length 30 m, in-

ternal diameter 0.25 mm, film thickness 0.25 μm) with secondary ionization in a collision cell with nitrogen with the collision energy 10 eV, to confirm the identification of individual compounds (Fig. S3). In addition, chromatograms of extract samples were obtained in the MRM (multiple reaction monitoring) mode on the SCION 436 GC TQ instrument, also to confirm the results of identification of individual compounds (Fig. S4) with secondary ionization in a collision cell with argon (collision energy 10eV), with controlling the following transitions: M<sup>+</sup> = 410 a.m.u. → 191, 189, 121, 367 (Shiojima et al., 1992; Ageta et al., 1994).

Components were identified using NIST 14 mass spectrometry libraries, as well as using a detailed study of the mass spectra of splinter ions and molecular ions using mass spectrometry reference literature, and also using rock samples and oil extracts previously analyzed in the laboratory, as well as standards provided by Chiron (hopenes).

The relative concentrations of the components were determined by the method of internal normalization relative to the total ion current (TIC) by dividing the area of the compound peak studied by the sum of the areas of all the peaks.

In the case of small peak areas and interference of neighboring peaks on the TIC chromatogram, individual compounds (alkylbenzenes, polyaromatic hydrocarbons) were normalized by dividing the corresponding peak areas of the mass fragmentograms of the corresponding characteristic ions ( $m/z$  91 for alkylbenzenes,  $m/z$  154, 178, 202 for polyaromatic hydrocarbons) on the sum of all *n*-alkanes peaks in the  $m/z$  57 mass fragmentogram. The reproducibility, which was calculated from parallel measurements, did not exceed 5%.

Blank experiments were performed to recognize and eliminate contaminants, which could penetrate into the samples during sampling, sample storage, extraction and concentration operations (Grosjean and Logan, 2007; Silva et al., 2013). In the present study, desulfurization of extracts was not applied, because the sulfur content was used as an additional tool for description and comparison of samples between themselves along with other biomarkers. Crystals of elemental sulfur for many samples were clearly visible in the extracts obtained from them.

**IRM-GC-MS.** The isotopic composition of organic carbon in samples of bottom sediments was measured on the DELTA V ADVANTAGE isotope mass spectrometer (manufactured by “Thermo Fisher Scientific”) connected to a Flash 2000 elemental analyzer using the ConFlo IV interface. Samples of bottom sediments were preliminarily decarbonated with hydrochloric acid. For each sample at least 3 parallel measurements were performed. The determination error did not exceed 0.20‰. The obtained values of carbon isotopic composition are given as  $\delta^{13}\text{C}$  values relative to the international standard VPDB.

The reliability of the measurement results was controlled by the IAEA standards — NBS-22 (mineral oil) with  $\delta^{13}\text{C}_{\text{VPDB}} = -30.03\text{‰}$  and IAEA-CH-7 (polyethylene  $\delta^{13}\text{C}_{\text{VPDB}} = -32.15\text{‰}$ ).

**Mineralogical fractional analysis.** The size composition of sedimentary material was studied on the laser diffraction analyzer “Analysette 22 Fritsch”. For different-grain sediments with inclusions of sand particles, the method of classical water-mechanical analysis combined with a laser analyzer was used (Petelin, 1961). The lithological (dimensional) typification of sedimentary substances was carried out on the basis of the three-component classification of the V.I. Il'ichev Pacific Oceanological Institute according to the ratio of the content of sand fractions (from 1 to 0.1 mm), aleurite fractions (from 0.1 to 0.01 mm) and pelite fractions (<0.01 mm) (Dudarev et al., 2016).

## RESULTS AND DISCUSSION

Tables 1–3, S2, S3 show the main parameters calculated from data of chromatography-mass-spectrometric analysis, as well as the parameters calculated on the basis of Rock-Eval pyrolytic analysis and  $\delta^{13}\text{C}$  isotopic analysis. Based on the parameters of IDM,  $\text{Pr}/\text{C}_{17}$ ,  $\text{Phy}/\text{C}_{18}$  (Table 1),  $\text{K}_i$  (Table 2), samples of the bottom sediments are characterized by

a low degree of diagenetic transformation (high values of IDM and relatively low  $\text{Pr}/\text{C}_{17}$ ,  $\text{Phy}/\text{C}_{18}$ ,  $\text{K}_i$ ). The IDM values range from 0.34 to 0.44 and are similar to the boundary values of this index between the coccolith and sapropel silts of the Black Sea (Melenevskii et al., 2017). However, for samples of group I, in which there is a significant predominance of the terrigenous signal, the degree of diagenetic maturity, based on the aforementioned coefficients, is higher (Fig. 4a, b).

The content of total organic carbon (TOC) in sediment samples in the polygon is generally low, reflecting the low bio-productivity of the Laptev Sea (Vetrov and Romankevich, 2004), which, in our opinion, is explained by: 1) low transparency of waters caused by high content of humic acids coming from the river runoff (Pugach et al., 2015, 2018), 2) a low proportion of OC of terrigenous origin, and relatively labile OC of marine origin due to its remoteness from the coastline (Tesi et al., 2014; Vonk et al., 2014; Bröder et al., 2016), 3) the high lability of the OC of marine origin, its proportion being predominant in this part of the Laptev Sea (Semiletov, 1999; Semiletov et al., 2011, 2012). With an increase in TOC content, the proportion of volatile organic substances (peak S1) and the proportion of degraded compounds above 300 °C, which belong to the class of biogeopolymers (protokerogen) (peak S2), also increase (Figs. S1, S2).

The HI parameter characterizes hydrogen saturation of the organic matter, and reflects the proportion of the aliphatic component in the structure of organic matter (OM). Several samples are characterized by increased values of the HI index (exceed the value of 100, Table 2), which means that they were formed in more reducing environment. The  $\delta^{13}\text{C}$  values of bottom sediment samples are close to each other and belong to the range of  $-23.0$ ;  $-24.9\text{‰}$  and are characteristic values for the studied area of the outer shelf (Tesi et al., 2014, 2016; Dudarev et al., 2016). These data are comparable with the  $\delta^{13}\text{C}$  data obtained for the samples collected from the estuaries of the GRARs (Great Russian Arctic Rivers), in particular, for the sediments collected from the Lena river estuary, the value was  $-25\text{‰} \pm 0,1\text{‰}$  (van Dongen et al., 2008; Semiletov et al., 2011; Feng et al., 2015), and for the samples of surface sediments collected from the Buor-Khaya Bay  $\delta^{13}\text{C}$  values were in the range of  $-25,3$ ;  $-27,5\text{‰}$  (Semiletov, 1999; Karlsson et al., 2011). The values that we obtained are “on the edge” of a significant effect of the influx of terrigenous carbon and shifted towards marine organics, since  $\delta^{13}\text{C}$  values of the organic carbon of terrigenous origin on average are  $-25\text{‰}$ , and the range characteristic for terrigenous organic matter ranges from  $-25\text{‰}$  to  $-30\text{‰}$  (Galimov, 1982; Semiletov, 1999). The relative content of *n*-alkanes with different numbers of carbon atoms in a molecule allows determining the type of bio-producer and the conditions of its fossilization (Tissot and Welte, 1984; Petrov, 1987). All samples are characterized by the predominance of *n*-alkanes containing an odd number of carbon atoms in the molecule, which are generally accepted markers of higher terrestrial vegetation (Fig. 2). It is considered that

**Table 2.** The geochemical coefficients and results of the Rock-Eval analysis of the bottom sediments

№ st.	The geochemical coefficients calculated on the basis of the GC-MS data						Rock-Eval parameters					$\delta^{13}\text{C}$ , ‰
	A/B	C/D	$K_i$	Pr/Phy	CPI	TAR	TOC, wt. %	S1 mg/g	S2	HI	MinC, wt. %	
20b <sup>1</sup>	0.55	3.05	0.29	2.61	8.04	1.85	1.01	0.23	0.82	81	0.18	–23.7
21m <sup>1</sup>	1.29	2.28	0.35	2.01	5.75	1.54	0.82	0.17	0.65	79	0.14	–24.1
22m	1.97	1.82	0.24	2.32	4.87	0.83	0.34	0.09	0.39	115	0.07	–24.4
23b	1.70	2.03	0.23	2.61	5.95	0.99	0.84	0.20	0.72	86	0.16	–24.3
25b	2.20	3.12	0.26	3.10	5.61	0.66	0.59	0.14	0.49	83	0.12	–24.3
28m	3.20	4.86	0.22	2.77	5.63	0.43	0.38	0.08	0.34	89	0.09	–24.5
29b	1.04	1.76	0.22	2.20	6.69	1.74	0.69	0.16	0.58	84	0.12	–25.2
30b	1.21	2.25	0.21	3.12	7.32	1.57	0.54	0.12	0.45	83	0.10	–23.8
32m	1.74	2.88	0.16	1.40	6.35	1.03	0.49	0.12	0.45	92	0.10	–24.4
33b	0.92	1.89	0.24	3.01	7.22	1.95	1.09	0.23	0.85	78	0.20	–23.2
34m	0.39	0.23	0.16	1.78	5.47	10.29	0.94	0.21	0.83	88	0.16	–23.4
35b	0.42	0.28	0.46	2.85	6.18	10.53	0.46	0.11	0.43	93	0.08	–23.0
36b	0.40	0.29	0.33	3.60	6.99	10.96	0.91	0.20	0.76	84	0.16	–24.5
37m	0.36	0.28	0.35	2.28	6.05	12.43	0.71	0.16	0.62	87	0.15	–24.6
38m	0.37	0.30	0.36	1.97	6.34	12.51	0.51	0.11	0.46	90	0.12	–24.6
40m	0.41	0.53	0.38	3.05	6.85	7.44	0.62	0.14	0.52	84	0.15	–24.2
43m	0.41	0.42	0.31	2.03	7.02	9.47	0.31	0.07	0.36	116	0.08	–25.2
44m	0.71	0.14	0.35	3.57	1.91	12.64	0.35	0.10	0.43	123	0.06	–25.5
45b	0.40	0.49	0.34	2.24	6.85	8.00	0.84	0.19	0.80	95	0.17	–24.5
48b	0.44	0.41	0.31	2.89	5.67	8.69	0.86	0.22	1.02	119	0.16	–24.3
49b	0.39	0.22	0.32	1.95	5.51	13.48	0.88	0.17	0.72	82	0.14	–24.9

Note. The sample number corresponds to the sampling station number. <sup>1</sup>m, designation of the station where methane emission is detected (Fig. 10, 12), b, designation of the sampling station beyond methane emissions zones. A/B, the ratio of the sum of the peak areas of *n*-alkanes over the even envelope to the sum of the peak areas of high molecular *n*-alkanes (markers of higher terrestrial vegetation) on *m/z* 57 chromatograms (Fig. 2a). C/D, the ratio of the sum of the peak areas of low-molecular *n*-alkanes to the sum peak areas of high-molecular alkanes over the even envelope curve on *m/z* 57 chromatograms (Fig. 2b).  $K_i = (\text{Pr} + \text{Phy})/(\text{nC}_{17} + \text{nC}_{18})$ . Pr/Phy, pristane-phytane ratio.  $\text{CPI} = 0.5 \cdot [(\text{C}_{25} + \text{C}_{27} + \text{C}_{29} + \text{C}_{31} + \text{C}_{33}) / (\text{C}_{24} + \text{C}_{26} + \text{C}_{28} + \text{C}_{30} + \text{C}_{32}) + (\text{C}_{25} + \text{C}_{27} + \text{C}_{29} + \text{C}_{31} + \text{C}_{33}) / (\text{C}_{26} + \text{C}_{28} + \text{C}_{30} + \text{C}_{32} + \text{C}_{34})]$ . TAR, terrigenous to aquatic ratio =  $(\text{C}_{27} + \text{C}_{29} + \text{C}_{31}) / (\text{C}_{15} + \text{C}_{17} + \text{C}_{19})$ . TOC, total organic carbon, wt.%. S1, the number of the low-boiling organic compounds (up to 300 °C), mg/g sediment (Fig. S1). S2, the number of the volatile products of the organic matter destruction, mg/g sediment (Fig. S1). HI, hydrogen index S2:100/TOC, mg products of the organic matter destruction / g organic carbon. MinC, total mineral carbon, wt.%.

the maximum in their distribution falls on  $\text{C}_{27}$ ,  $\text{C}_{29}$ ,  $\text{C}_{31}$  (Eglinton et al., 1962; Smith et al., 2007; Volkman et al., 2015). It is worth noting that there is rather high content of  $\text{C}_{31}$  alkane in the composition of the high molecular weight *n*-alkanes in all samples, which is a marker of sphagnum moss that grows in marshy coastal bays (Romankevich et al., 2003; Tesi et al., 2014).

The odd index CPI in all samples has high values, which indicates a constant flow of fresh biogenic material from the continent to sediments by the river runoff, for example, the CPI index > 5 is characteristic of modern higher terrestrial vegetation (Rieley et al., 1991; Hedges and Prahl, 1993).

Alkanes with an even number of carbon atoms are present on the chromatograms along with odd *n*-alkanes. However, their origin is difficult to explain unequivocally, since they can represent both the contribution of marine (phytoplankton) and the bacterial component of organic matter, as

well as indicate the presence of the oil component of OM (Petrov, 1987; Peters et al., 2005), which, in turn, may be due to products coming from deeper horizons as a result of upward migration. A lower value of CPI (1.91) was recorded for one station (№ 44, located in the methane seep zone). Similar ratio is typical for oils, for example, for *n*-alkanes of Norman Wells oils, it is 1–2 (Petrov, 1987; Romankevich et al., 2003), as well as for the sediments of the Mackenzie River estuary, where CPI values range from 1.8 to 2.7, due to petrogenic influence, since there are oil and bitumen deposits in the basin of this river (Yunker et al., 1993, 1995, 2002; Drenzek et al., 2007). It is also important to note the presence of biphenyl in samples of station № 44 (Table 3), since at stations 34–49 it is missing. Therefore, it is likely that there may be a hydrocarbon influx for this station. Siterols, cholesterol, small amounts of stigmaterol (*m/z* 213) and oleanan (*m/z* 191, Fig. 8) identified in most samples and

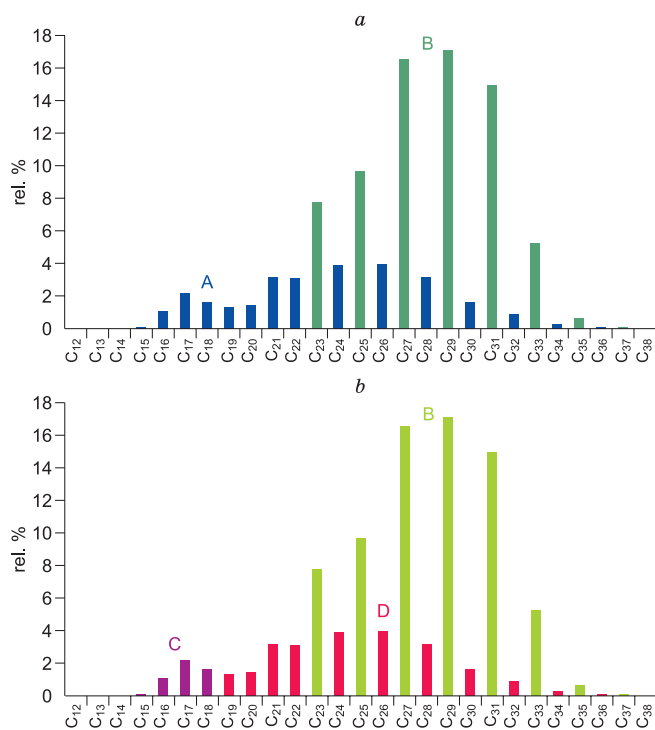


**Fig. 2.** Molecular weight distribution of *n*-alkanes (sample № 49). Scheme for calculating A/B and C/D parameters is shown. a) A, the sum of *n*-alkane peaks on the even envelope (highlighted in blue); B, the sum of the peaks of high-molecular *n*-alkanes, which are markers of land plants, on the odd envelope – C<sub>23</sub>, C<sub>25</sub>, C<sub>27</sub>, C<sub>29</sub>, C<sub>31</sub>, C<sub>33</sub>, C<sub>35</sub>, C<sub>37</sub> (highlighted in green). b) C, the sum of the peaks of low-molecular *n*-alkanes on the even envelope C<sub>12</sub>–C<sub>18</sub> (highlighted in purple); D, the sum of the peaks of high-molecular *n*-alkanes on the even envelope C<sub>19</sub>–C<sub>38</sub> (highlighted in red).

also originated from higher terrestrial vegetation are additional markers of the terrigenous signal (Tissot and Welte, 1984; van Dongen et al., 2008).

Polyaromatic hydrocarbons (PAHs) were identified in quite large quantities relative to *n*-alkanes in the sediments. The origin of PAHs can be related to the migration of petroleum hydrocarbons, including their transport by the Lena River, since numerous of oil-saturated rock outcrops are noted along the coasts of the Eastern Siberia Rivers and on the coastline of the continent (Kashirtsev, 2003; Kashirtsev et al., 2004, 2013). However, the remoteness of the study area from the Lena River delta (over 450 km) can be a reason to consider this factor as insignificant. Positive trends of these compounds relative to each other over the entire polygon area regardless of the presence or missing of the methane seeps (Fig. 3) indicate that they have one formation source. On the other hand, this preliminary conclusion is uncertain, since these compounds could also be formed as a result of the marine biota activity and the cyclization process of polyunsaturated fatty acids in reducing marine environment (Goncharov, 1987; Fahl and Stein, 1997).

The presence of biphenyl, which is typically a petroleum product, reinforces our suggestion about the migration na-

ture of petroleum hydrocarbons in the study area. Correlations of biphenyl content relative to other PAHs look less significant (Fig. 3b, d, f), which may be additional evidence in favor of another source of this compound. It can be assumed that the part of biphenyl could have been formed due to oxidative destruction from phenanthrene (Sun and Puttmann, 2001). The absence of this compound at about half of all stations, which are located mainly in the western part of the investigated polygon (Fig. 10; Table 3) and where the investigated sediment samples were collected, still remain unclear. We suppose that this may be due to the high mosaic pattern in the distribution of gas streams (Shakhova et al., 2015; Leifer et al., 2017), where the signal of upward migration of petroleum hydrocarbons should be expressed most clearly. This question requires further clarification on the basis of a complex of geophysical and biogeochemical methods that are planned for sea expeditions in 2020–2021.

We used the A/B and C/D coefficients to characterize the composition of *n*-alkanes and to assess the contribution of the marine OC relative to the terrigenous OC (Fig. 4a; Table 2). The C/D coefficient characterizes the relative concentration of low molecular weight *n*-alkanes, which refer to the source of marine organic carbon and originate from phytoplankton and bacteria (Fahl and Stein, 1997), while the A/B coefficient characterizes the proportion of *n*-alkanes by the even envelope of the *n*-alkane distribution relative to high molecular weight *n*-alkanes, which are the markers of higher terrestrial vegetation. In fact, this coefficient characterizes the contribution of the marine organic carbon relative to the terrigenous OC [Han and Calvin, 1969; Ladygina et al., 2006; van Dongen et al., 2008]. This is indirectly confirmed by the positive correlation between the parameters A/B and C/D (Fig. 6a).

Thus, the studied samples are divided into two groups (Fig. 4a, b). In samples belonging to the first group (I), the contribution of the terrigenous OC predominates, and in the second group (II), the influence of the marine OC is already more significant (on average, TAR is an order of magnitude higher for the first group, see Table 2). The maximum of marine origin OC is accumulated at station 28, which is located as more “marine” in relation to the two designated groups on the graph (Fig. 4a) and has a minimum TAR index (0.43). It is worth noting that that the average value of  $\delta^{13}\text{C}$  of the second group (–24.19‰) is slightly higher compared with the first group (–24.43‰). The second group of the samples (“marine”) on average is characterized by lower values of the coefficients  $K_i$ , Pr/C<sub>17</sub>, Phy/C<sub>18</sub> and higher IDM values compared with the samples of group I (Tables 1, 2), which characterizes the increased contribution of less diagenetic transformed OM of marine origin into sediments of the second group, as terrigenous OM undergoes more diagenetic transforming during transportation (Tesi et al., 2014, 2016; Bröder et al., 2016). Furthermore, the concentration of alkylbenzenes and PAHs is significantly higher for the samples of the second group (Table 3), which confirms the presence of a significant contribution of the OC of

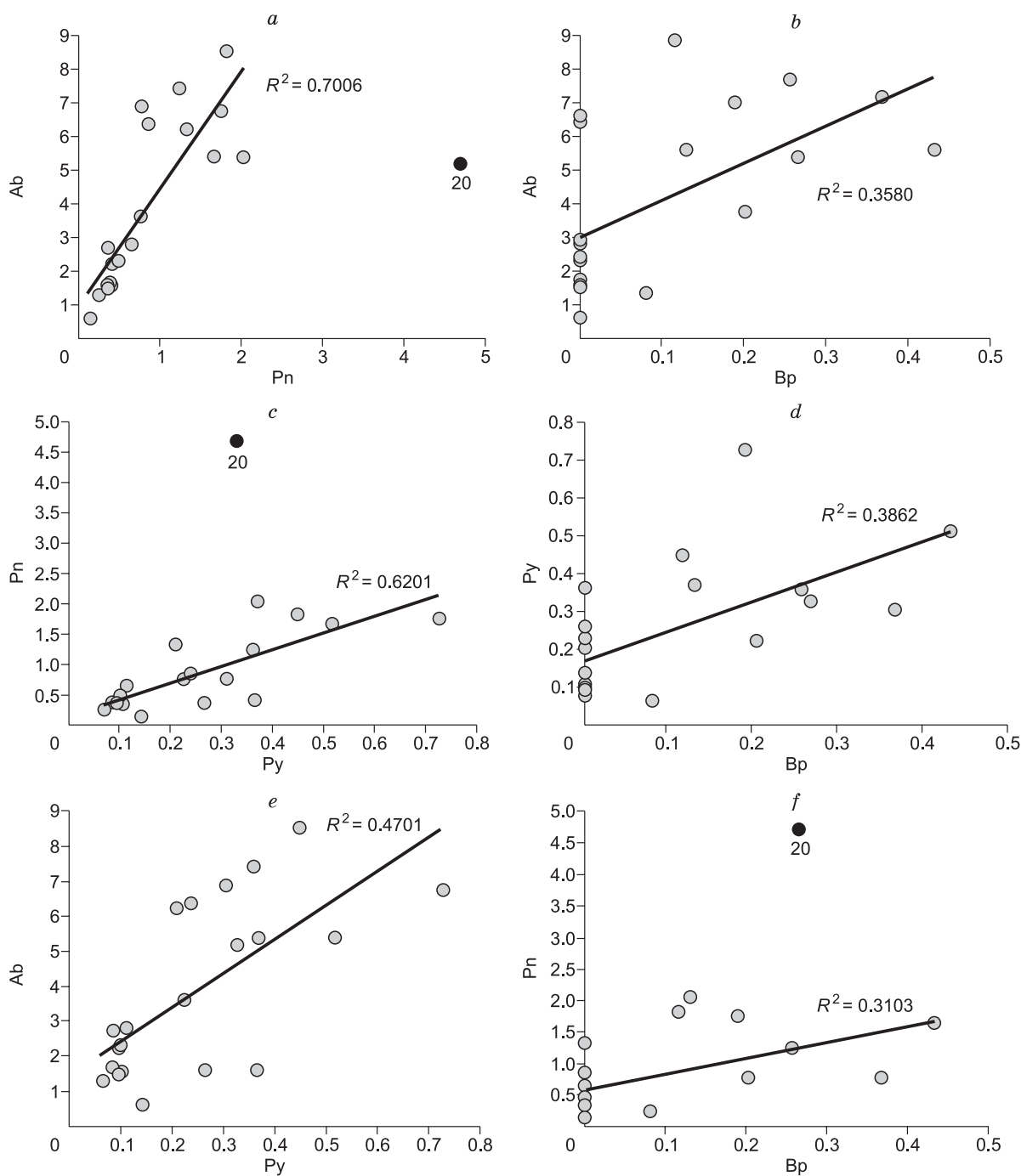


**Fig. 3.** Dependence between the contents of aromatic hydrocarbons over the entire area of the investigation polygon. The sample of station № 20 falls out from the detected trends (see graphs *a, c, f*).

hydrobionts to the sediments of this group (Petrova et al., 2008, 2010; Goncharov, 1987). The ratio of the alkylphenanthrenes to the phenanthrene (APn/Pn) is reduced for all stations ( $<1$ ) (Table 3), which indicates a relatively high transformation of organic matter of the sediments (according to (Petrova et al., 2008), this coefficient is 2.5 for the ESS sediments). The ratio APn/Pn on average is higher at the “marine” stations. The same division of the samples into

two groups is observed when building the dependencies of the following identified compounds in the sediments D: A-Friedolean-6-ene (FO), oleanane (OI) as well the OEP oddness index (Table S4) relative to the TAR index (Figs. S10, S13). FO and OI have terrigenous origin from higher terrestrial vegetation (Peters et al., 2005) and FO increases from the “marine” group of samples (II) to the “terrigenous” group (I) (Fig. S10a), with the average content of FO at ter-

**Table 3.** The relative concentrations of the aromatic hydrocarbons, squalene, and sulfur in bottom sediments

Sample №	Component concentration, % rel. to the sum of the peak areas of <i>n</i> -alkanes by m/z 57					Component concentration, % rel. to the sum of all peak areas	
	Ab	Bp	Pn	Py	APn/Pn	S	Sq
	m/z 91	m/z 154	m/z 178	m/z 202	m/z(192+206)/178	m/z 64	m/z 69
20b	5.19	0.27	4.70	0.33	0.75	6.30	n.d
23b	5.41	0.43	1.67	0.52	0.80	3.40	0.01
25b	8.54	0.12	1.82	0.45	0.59	10.36	0.01
29b	6.21	0.01	1.33	0.21	0.52	21.80	n.d.
30b	3.63	0.20	0.78	0.22	0.57	7.05	n.d.
33b	6.38	0.01	0.86	0.24	0.32	14.00	0.01
35b	1.59	n.d.	0.36	0.27	0.41	16.36	0.66
36b	1.59	n.d.	0.41	0.37	0.54	27.70	1.80
45b	2.79	n.d.	0.66	0.11	0.25	30.80	0.43
48b	2.32	n.d.	0.49	0.10	0.53	24.60	n.d.
49b	1.46	n.d.	0.36	0.10	0.75	15.45	n.d.
Avb	4.10	0.17	1.22	0.27	0.55	16.17	0.49
21m	5.39	0.13	2.03	0.37	0.57	0.60	n.d.
22m	6.75	0.19	1.75	0.73	0.62	1.03	0.01
28m	7.42	0.26	1.24	0.36	0.59	16.17	n.d.
32m	6.91	0.37	0.78	0.31	0.40	24.31	n.d.
34m	0.61	n.d.	0.14	0.14	0.48	30.06	0.42
37m	1.66	n.d.	0.38	0.08	0.34	26.00	4.19
38m	1.54	n.d.	0.35	0.10	0.66	33.20	1.29
40m	2.73	n.d.	0.37	0.09	0.64	25.70	1.10
43m	2.24	n.d.	0.41	0.10	0.54	23.20	1.78
44m	1.29	0.08	0.26	0.07	0.27	29.00	0.45
Avm	3.65	0.21	0.77	0.24	0.51	20.93	1.32

Note. Sq, squalene; S, elemental sulfur ( $S_6+S_8$ ); Ab, phenylalkanes with a small admixture of linear *n*-alkylbenzenes (Fig.7); Bp, biphenyl; Pn, phenanthrene; Py, pyrene; APn/Pn, the ratio of the content of the sum of methyl phenanthrenes and dimethylphenanthrenes to the content of holonuclear phenanthrene; n.d., the analytical signal of the compound is not determined. Avb, the average concentration of the components at the sampling stations beyond methane seepage zones; Avm, the average concentration of the components at the sampling stations in the methane seepage zones.

terrestrial stations being 1.8-fold higher. The same trend could be expected in the case of oleanane, however, such correlation is not observed (Fig. S10b), possibly due to the inflow of oleanane not only in the course of transportation of the erosional and river OC to sediments, but also from deeper horizons with ancient OC as a result of degradation of subsea permafrost (Semiletov et al., 2007; Salvado et al., 2016; Shakhova et al., 2017). Nevertheless, it is worth noting that the oleanane average content in the terrigenous group is 1.2-fold higher than that in the marine group. The graphic distribution of the TAR index by the sampling stations is shown in Fig. 7, and C/D is shown in Fig. S14. It can be seen that the most of marine stations with low TAR index and high C/D index are confined mainly to the eastern part of the polygon.

Alkylbenzenes (Ab) found in the studied sediments are mainly represented by phenylalkanes (Fig. 5) (Peters et al., 2005). Phenylalkanes are presumably biomarkers of marine microbiota (including archaea) (Kristjansson et al., 1982; Lengeler et al., 1999; Peters et al., 2005). Ab are markers of

marine organic carbon, since they positively correlate with the parameters A/B and C/D (Fig. 6). On the other hand, for these components an additional contribution from technogenic source is not excluded (Eganhouse, 1986; Ellis et al., 1996; Peters et al., 2005). In contrast, phenylacetic acid esters (Bae, Fig. 6), also detected by m/z 91, are likely to have terrigenous origin from higher terrestrial vegetation (Wightman and Lighty, 1982) (Fig. 5).

Squalene, which is a common marker for all domains of living organisms (Peters et al., 2005), was detected in the sediments of the investigated polygon in different concentrations. In the case of marine origin of the OC, the most likely sources of the squalene are eukaryotes, bacteria (Donk, 2015) or archaea (Matsumoto and Watanuki, 1990). Squalene is also characteristic of diatoms (Matsueda et al., 1986). Its terrigenous sources are mainly microorganisms and higher terrestrial vegetation (Tissot and Welte, 1984). As follows from Table 3 and Fig. 4, squalene is practically missing in samples conditionally belonging to group II, which may testify in favor of its more terrigenous origin.

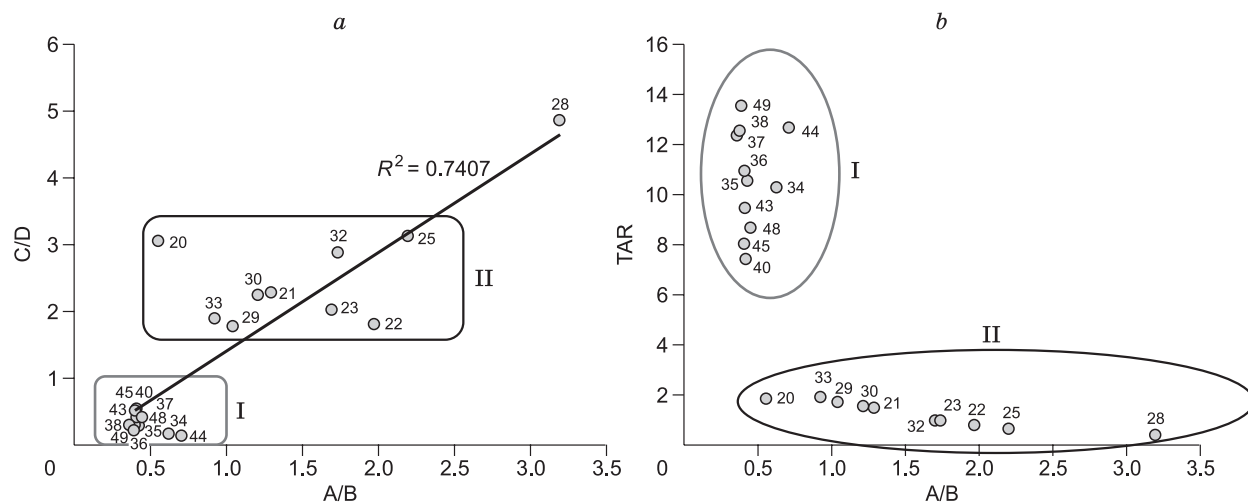


**Fig. 4.** Dependence of the parameter C/D on the parameter A/B (a) and dependence of the parameter TAR (terrigenous to aquatic ratio) on the parameter A/B (b). The numbers indicate sampling stations. Roman numerals denote groups of the samples: I, with the predominance of the terrigenous OC; II, with the increased contribution of the marine OC.

Interesting inverse regularity is observed for the squalene relative to the biphenyl: starting from sample station 34, there is a decrease in the concentration of the biphenyl, while the content of squalene increases. This means that biphenyl was formed at stations enriched with marine organic matter, therefore, it could originate from deeper sedimentary horizons (Belenitskaya, 2012), where oil and gas fields are supposed to be present (Malyshev et al., 2010; Safronov et al., 2013; Vinogradov et al., 2013).

Hopanoids were identified in the composition of the investigated sediments (Dp, Hp17, Hp21, etc.) (Figs. 8, 9; Table S2, S3), and in this case they related to the organic matter of the marine origin (Blumenberg et al., 2010; Zhu et al., 2013; Rush et al., 2016), because no correlation was found between their content and TAR coefficient (Prah et al., 1992). Therefore, in this case, hopanoids, apparently, are biomarkers of bacteria acting in the water column and sediments. The source of the formation of these compounds resulting from diagenesis is bacteriohopanepolyols (bacteriohopanepentol, -tetrol, and -triol) and diplopterol (Dol),

which, in particular, are contained in the lipids of the methanotrophs bacteria (Rohmer et al., 1980; Simoneit, 2004; Medeiros and Simoneit, 2007; Rush et al., 2016). Bacteriohopanepolyols are contained in the membranes of aerobic bacteria (for example, cyanobacteria), heterotrophic and methanotrophic bacteria (Talbot et al., 2008, 2014, 2016; Cooke et al., 2009). C<sub>30</sub> hopanoids, such as Dol, diplopterol (Dp) are synthesized by the variety of bacterial species and mainly originate from aerobic bacteria in the oxidizing environment. However, it has recently been shown that various anaerobic bacteria can contain a range of hopanoid lipids including hop-22(29)-ene (Dp) и hop-21(22)-ene (Hp21) (Damste et al., 2004, 2014; Fisher et al., 2005; Hartner et al., 2005).

The neohop-13(18)-ene (nHp), detected in the collected sediments in the course of the research, is a rearranged hopene, its carbon skeleton is identical to that of the hopanes, but the methyl group is located at C-17 instead of C-18 (Fig. 9) (Moldowan et al., 1991; Damste et al., 2014). The rearranged hopenes were previously found in modern and

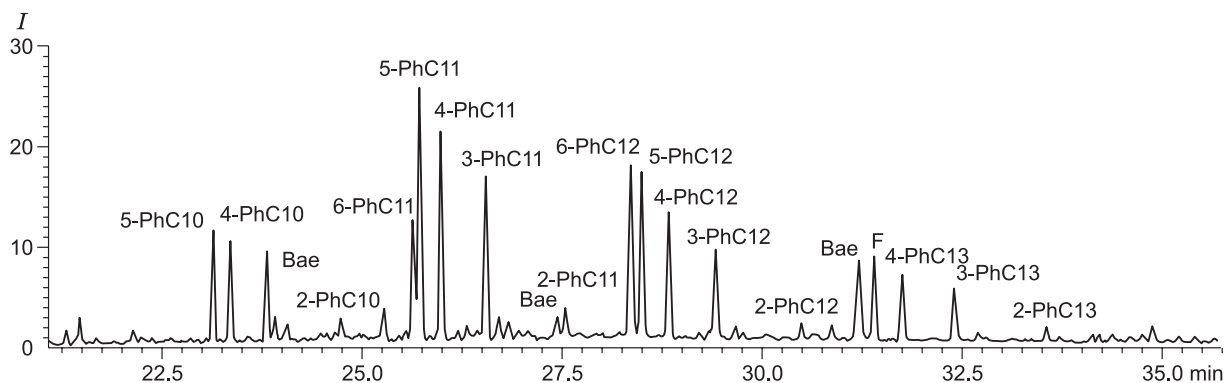


**Fig. 5.** Chromatogram (m/z 91) of sample extract № 33: Ph, the designation of a phenyl radical; Bae, esters of phenylacetic acid; F, phthalate.

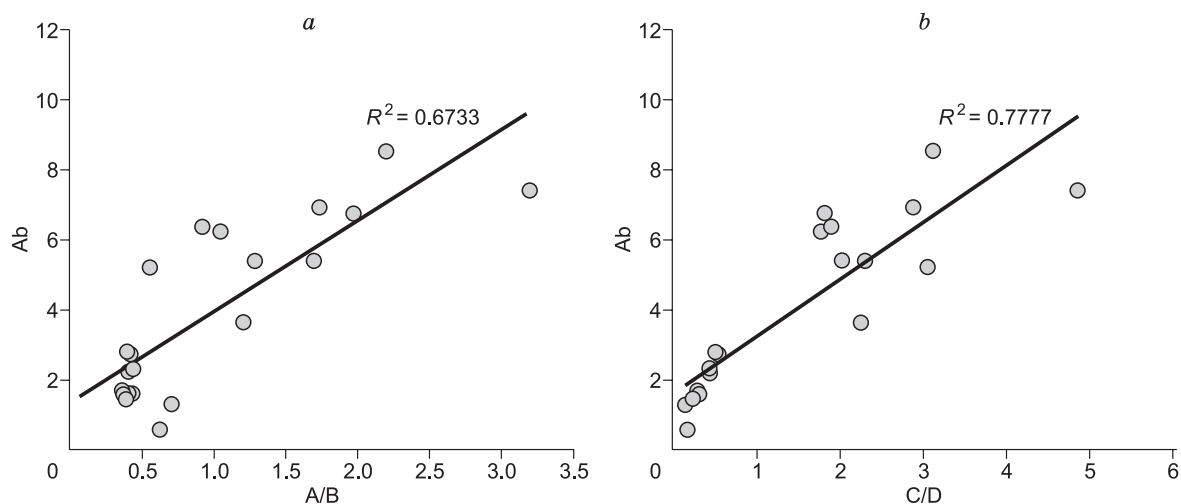


Fig. 6. The dependence of the Ab content on the parameters A/B (a) and C/D (b) over the entire area of the polygon.

ancient sediments, both marine and lacustrine (Brassell and Farrimon, 1986; Stein et al., 1988; van Dongen et al., 2006a,b). These compounds can be formed through dehydrogenation and isomerization reactions from the quite common hopanols and hopenes.

The identified  $C_{30}$  hopanoids, as mentioned above, are derived from bacteriohopanepolyol (probably from aminopentol (Volkman et al., 2015; Osborne et al., 2017)), and further in the process of diagenesis diploptene (Dp), hop-21(22)-ene (Hp21), hop-17(21)-ene (Hp17), neohop-13(18)-ene (nHp) are formed as a result of dehydration and isomerization processes, and as a result of the hydrogenation of these isomers hopane  $\beta\beta C_{30}$  ( $\beta H30$ ) is formed and then as a result of diagenesis hopane  $\alpha\beta C_{30}$  (H30) is formed. This chain of diagenetic transformations is characteristic of lipids of methanotrophic microorganisms, as was shown in (Volkman et al., 2015, Fig. 5).  $C_{30}$  Ts hopane was not detected in the samples collected, and in general, it is not found in sediments and oils, but its precursor neohop-13(18)-ene, detected in the analyzed samples was also found in a number of other sediments (Damste et al., 2014; Volkman et al., 2015).

It is noteworthy that the abnormal amount of diploptene isomer hopene  $C_{30}$  (Uh, Figs. 8, 9) is present in the OM of the sediments, which has hardly been described in the previous works. The average content of this hopene at the “methane” stations is 1.4-fold higher than that at the “background” stations, and the average content of the sum of  $C_{30}$  hopenes at the methane stations is twice as high as that at the background ones.

In addition to the abovementioned hopenes, biological  $\beta\beta$ -hopanes  $C_{29}$ ,  $C_{30}$ ,  $C_{31}$ , geohopanes –  $\beta\alpha$ -hopanes  $C_{29}$  and  $C_{30}$  (moretane), as well as  $\alpha\beta$ -hopanes  $C_{29}$ ,  $C_{30}$ ,  $C_{31}$ , and  $C_{32}$  (S and R epimers) were detected (Fig. 8; Tables S2, S3), which are also products of the diagenetic chain of transformations of bacteriohopanepolyol (Damste et al., 1995; Volkman et al., 2015). Tm, H29,  $\beta\alpha$ -hopanes, Tm-ene and T $\beta$  compounds may have the same origin (Fig. 8). Tm, H29,  $\beta\alpha H29$ , H30, M,  $\alpha\beta H31S$  and  $\alpha\beta H31R$  components may occur both in sedimentary rocks and in oils, but Ts (it was detected in most samples in trace amounts by MRM method),  $\alpha\beta H32S$  and  $\alpha\beta H32R$  have only petroleum origin, therefore detection of these hydrocarbons may suggest the inflow of the oil OM (“micro-oil”) through thawed permafrost into the sediments (Wenger et al., 2002). It should be noted that the average concentration of  $C_{32}$   $\alpha\beta$ -hopanes in the zones of the methane seeps is 1.5-fold higher compared to the “background” stations. Also, it is likely that due to the inflow of the OM of petroleum origin, we observe the increase in H30 content (1.5 times higher at the seep stations on average) and at the same time the decrease in the M/(M+H30) index relative to the hopane index  $C_{31}$  S/(S+R) (Fig. S8; Table S4). Coupled with the detection of the trace quantities of the steranes ( $\beta\beta$ -steranes, Fig. S16) and Ts, the average 1.2-fold increase in the content of alkanes on the even (“oil”) envelope (Goncharov, 1987) in the molecular weight distribution of the *n*-alkanes (the A/B coefficient) at the stations with methane emissions also indicates the possible inflow of the OM of oil origin (Fig. S13). Here it is worth noting that the

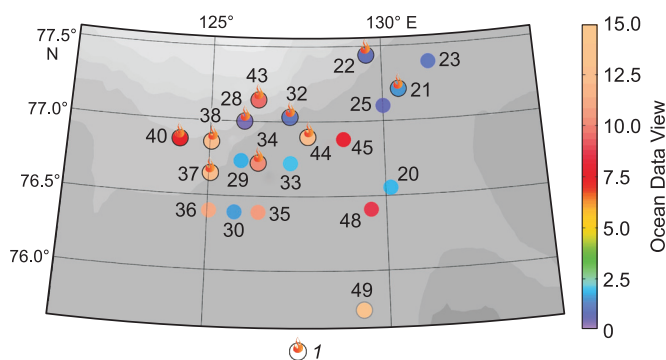
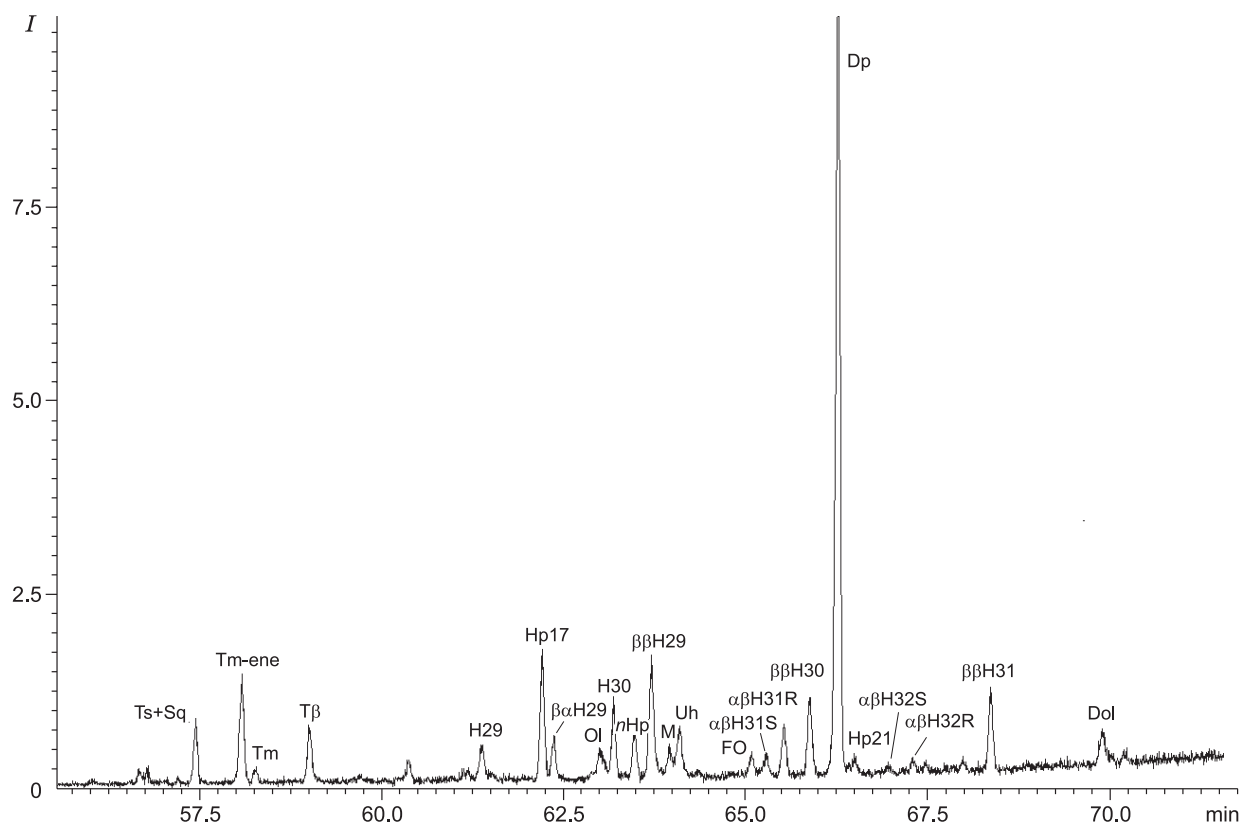


Fig. 7. Distribution of TAR index values over the area of the investigation polygon. The numbers indicate sampling stations. The map was created using the Ocean Data View software. Number 1 designates the stations that are located in the methane seep area.



**Fig. 8.** Chromatogram ( $m/z$  191) of sample extract № 40: Sq, squalene; Ts, 18 $\alpha$ (H)-22, 29, 30-trisnorhopane; Tm-ene, 17 $\alpha$ (H)-22, 29, 30-trisnorhop-(17,21)-ene; Tm, 17 $\alpha$ (H)-22, 29, 30-trisnorhopane; T $\beta$ , 17 $\beta$ (H)-22, 29, 30-trisnorhopane; H29, 17 $\alpha$ (H), 21 $\beta$ (H)-30-norhopane; Hp17, C<sub>30</sub> hop-17(21)-ene;  $\beta\alpha$ H29, 17 $\beta$ (H), 21 $\alpha$ (H)-30-norhopane (normoretane); OI, oleanane; H30, 17 $\alpha$ (H), 21 $\beta$ (H) C<sub>30</sub> hopane; nHp, C<sub>30</sub> neohop-13(18)-ene;  $\beta\beta$ H29, 17 $\beta$ (H), 21 $\beta$ (H)-30-norhopane; M, 17 $\beta$ (H), 21 $\alpha$ (H)-hopane (moretane); Uh, unknown C<sub>30</sub> hopene; FO, D:A-friedolean-6-ene;  $\alpha\beta$ H31S and  $\alpha\beta$ H31R, C<sub>31</sub> 17 $\alpha$ (H), 21 $\beta$ (H) homohopanes 22S and 22R epimers respectively;  $\beta\beta$ H30, C<sub>30</sub> 17 $\beta$ (H), 21 $\beta$ (H)-hopane; Dp, diploptene (C<sub>30</sub> hop-22(29)-ene); Hp21, C<sub>30</sub> hop-21(22)-ene;  $\alpha\beta$ H32S and  $\alpha\beta$ H32R, C<sub>32</sub> 17 $\alpha$ (H), 21 $\beta$ (H) bishomohopanes 22S and 22R epimers respectively;  $\beta\beta$ H31, C<sub>31</sub> 17 $\beta$ (H), 21 $\beta$ (H)-homohopane; Dol, diplopterol (hopan-22-ol).

S/(S+R) C<sub>32</sub> index is characteristic in its values for the mature OM of petroleum origin (Table S4). Possibly due to the uneven inflow of micro-oil to the OM of the sediments, we cannot observe clear correlations for the Tm component and C<sub>31</sub> and C<sub>32</sub>  $\alpha\beta$ -hopanes components relative to the pelitic fraction (Fig. S6).

Furthermore, we note that in the sediments collected at different times outside the investigated polygon  $\alpha\beta$ C<sub>32</sub>-hopanes, diplopterol, hop-21(22)-ene and Uh are missing, and neohop-13(18)-ene, hop-17(21)-ene and diploptene are contained in significantly smaller quantities (Fig. S15). This indicates the missing of the OM inflow into the sediments associated with the methane release in total outside the investigated polygon.

The origin of methane in the research area is detected on the basis of three-isotope studies (<sup>13</sup>C, D, <sup>14</sup>C), which is a complicated task in general (Sapart et al., 2017). However, it can be argued that the large proportion of methane is produced in the sediment layer, with the thickness up to 5–10 km, and enters the bottom layer, where it can be partially oxidized by aerobic methanotrophic bacteria and anaerobic methanotrophs and methanotrophic archaea (Peck-

mann et al., 1999; Thiel et al., 2001; Savvichev et al., 2010). Methanotrophic microorganisms make the group of methylotrophs that use methane as the sole source of carbon and energy and are the most important link in the utilization of methane released into the atmosphere (Oremland and Culbertson, 1992; Hanson and Hanson, 1996). Methanotrophs are widespread and form communities, even under extreme conditions (Lein et al., 2000; Wagner et al., 2005; Savvichev et al., 2010).

The bubble mechanism of methane transfer dominates in the study area (Shakhova et al., 2015), which allows the main part of the rising gas to avoid oxidation and get into the water column and atmosphere (Sapart et al., 2017). However, over a long period of time in some parts of the bottom, besides bubble transfer, a diffusion mechanism of migration may be present, or complete dissolution of small bubbles (with a diameter of less than 2 mm) may take place, as it was previously observed in northern lakes (Semiletov et al., 1996). Therefore, the possibility of the development of the methanotrophs colonies in the seep areas of the Laptev Sea shelf (Fig. 10) is quite likely, by analogy with the bacterial mats found on the Gakkel Ridge near hydrothermal

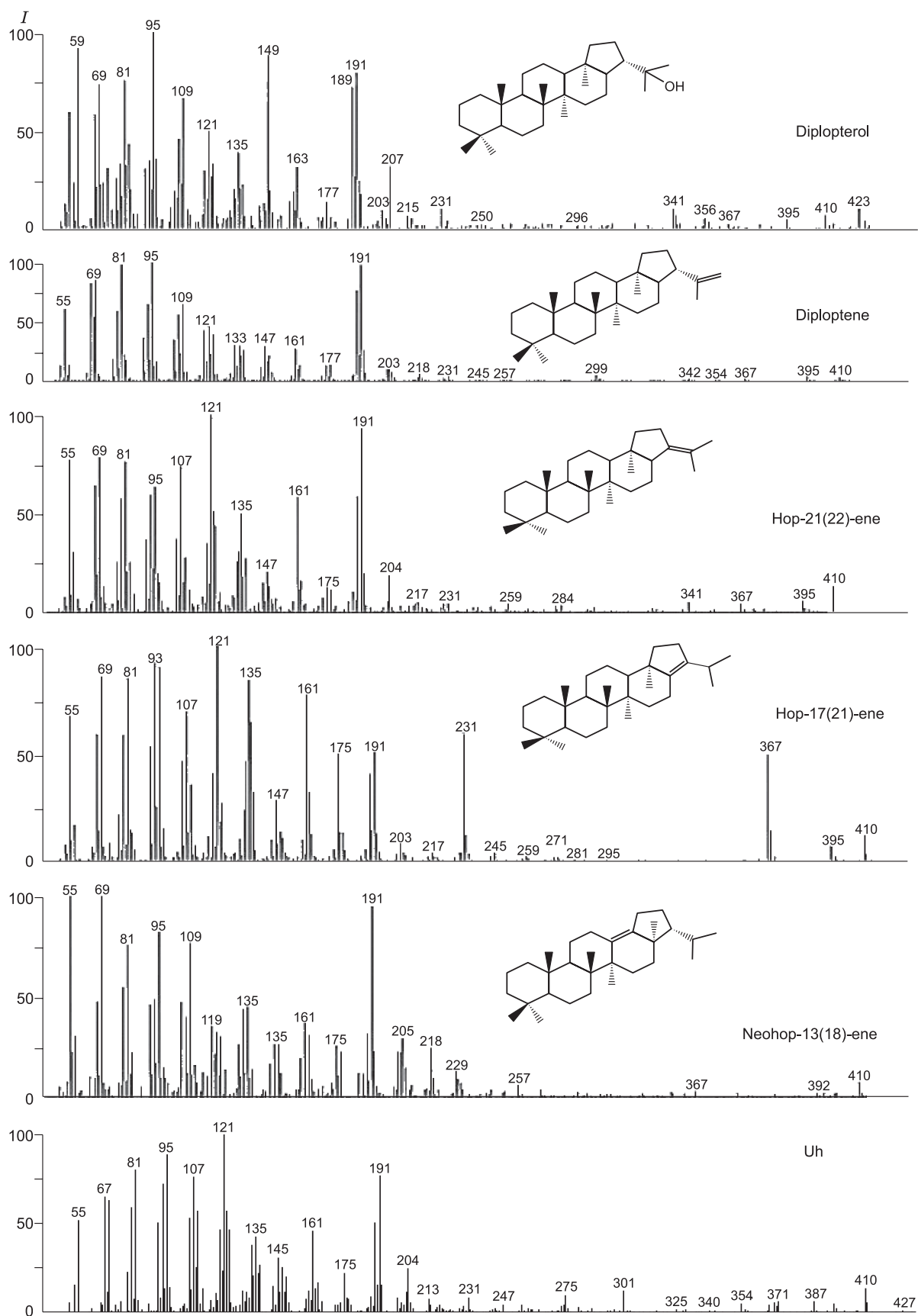


**Fig. 9.** Mass spectra of the individual identified hopanoids in the Laptev Sea sediments. Uh, unknown C<sub>30</sub> hopene.

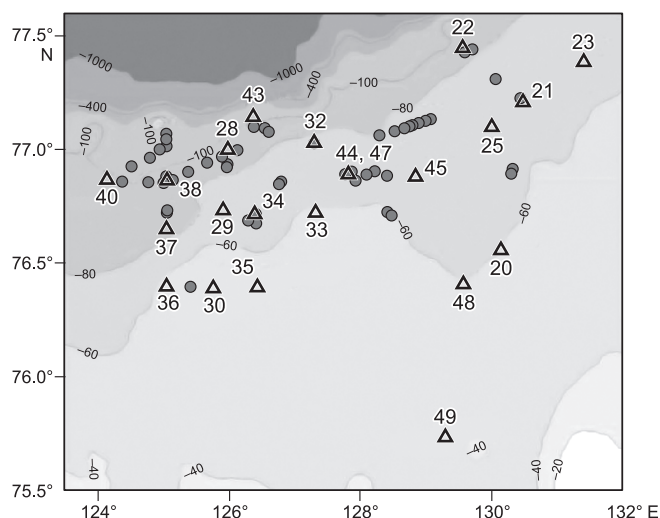


**Fig. 10.** The location of sampling stations (black triangles) and registered methane emissions (red circles) within the investigation polygon (Shakhova et al., 2015).

methane sources (Helmke et al., 2007; Thomas et al., 2008), which is confirmed by carbonate nodules found in the study area and supposed to be products of authigenic carbonate formation (Dudarev et al., 2016).

This assumption is confirmed by positive correlations of the concentrations of the abovementioned markers of the methanotrophs from the pelite fraction in the sediments (Tables S1, S2, S3; Fig. 11a) at the sampling stations in the areas of intense methane emissions (Fig. S6, Fig. 11a). It is worth noting here that such correlations are observed only for hopanoids, and for the remaining OM components (with the exception of alkanes and biogeopolymers, assessed by parameter S2) of the sediments such trends were not recorded. Organic matter is produced and sorbed on the surface of the fine pelite in the sediments left after the removal of its

part by methane flows and bottom currents (Fig. S5a). On average, the OC content in the areas of jet emission of methane is lower compared to the stations located outside the methane emission zones, which may be associated with a diluting effect, due to the filling of sediments with sand from deeper horizons and the removal of part of the fine pelite fraction (negative trend of the quantity of OC depending on the content of the sand fraction, see Fig. S5b, as well as (Dudarev et al., 2016; Panova et al., 2017). At stations outside the area of methane emissions, such trends are observed neither for TOC nor hopanoids relative to the mineralogical composition (more “quiet” regime of sedimentation) (Fig. S5c, d, Fig. S7, Fig. 11b). In general, for background stations we can even observe rather the reverse trend of hopanoids content relative to the pelitic fraction (Fig. 11b, Fig. S7), because of the lower production of these compounds at the stations outside the methane seeps and due to the dilution by the fine pelite fraction. The distribution of hopanoids concentrations over the area of the investigated polygon is clearly shown in Fig. 12.

From the foregoing, it can be concluded that at the “methane” stations there is a more intense activity of methanotrophic microorganisms compared to the background stations, and there is also a possibility of “micro-oil” inflow into the sediments. The average concentration of all identified hopanoids is 1.5-fold higher and squalene concentration is more than 2.5-fold higher at the methane stations than beyond the scope of these zones. This geochemical anomaly can be associated both with the activity of methanotrophs and with the inflow of OM from the underlying horizons, since in the deep (open) taliks, besides the intense methane bubbling (Sergienko et al., 2012; Shakhova et al., 2015, 2017), there is a probable discharge of the deep geofluid including oil components (V. Peresypkin, personal communication; Kasymuskaya et al., 2005; Overduin et al., 2007; Vonk et al., 2012).

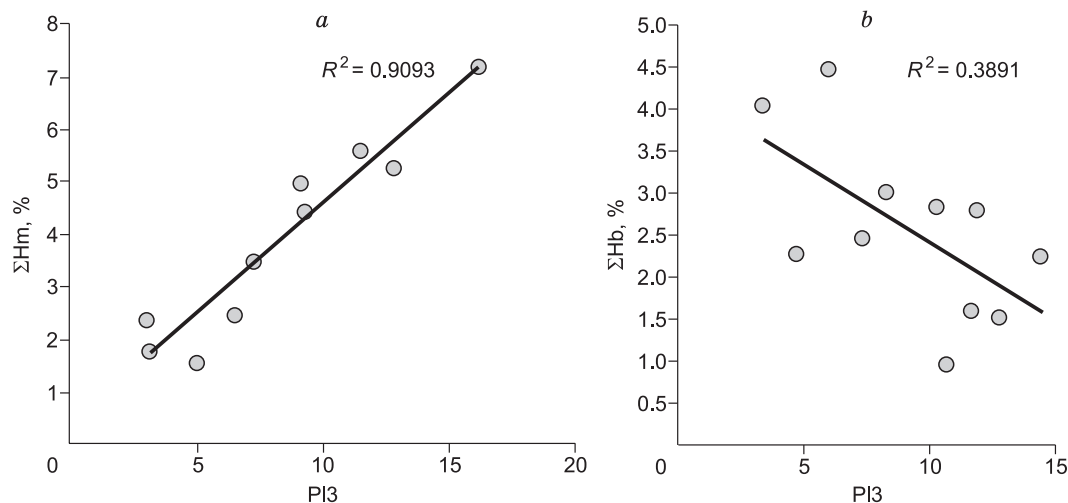


**Fig. 11.** Dependence of the total content of hopanoids ( $\Sigma H$ ) on the content of finely dispersed pelite fraction (PI3) in the sediments at stations in zones of the methane emissions (a) ( $\Sigma H_m$ ) and outside these zones (b) ( $\Sigma H_b$ ).

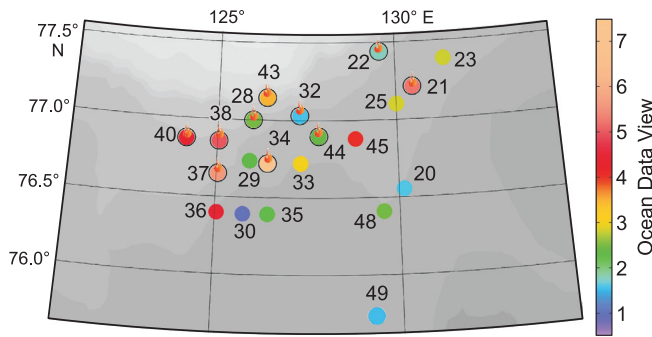


**Fig. 12.** Distribution of total relative concentrations of hopanoids ( $\Sigma H$ , %) over the area of the investigation polygon. Fire badges in the black circle indicate the station numbers in the zones of intense methane emissions.

It was also found that increased sulfur formation at the stations in the methane emissions zones (average content is 1.3-fold higher than that the stations located outside the jet transfer of methane) can be associated with more intensive processes of sulfate reduction in these areas. As is known, methanotrophs, which are active in the methane seeps, create the favorable environment for sulfate reducers in the community with methanotrophic archaea (Lein et al., 1996, 2000; Savvichev et al., 2010). The so-called anaerobic oxidation of methane takes place due to biological filter widespread throughout the World Ocean (Michaelis et al., 2002; Joye et al., 2004; Cooke et al., 2009; Knittel and Boetius, 2009; Timmers et al., 2016). Thus, methane in the areas of its outflow is consumed not only by aerobic methanotrophs (de Angelis et al., 1991; Lein et al., 2000), but also undergoes anaerobic oxidation by a consortium of sulfate reducers and methanotrophic archaea, with the latter process being more intense (Aloisi et al., 2002; Joye et al., 2004). These processes can contribute to the formation of authi-

genic carbonate mineral deposits found in the investigated polygon (Aloisi et al., 2002; Lein, 2009; Dudarev et al., 2016). It is possible that the colorless sulfur bacteria may additionally contribute to the accumulation of elemental sulfur in the sediments of the methane seeps (Dworkin et al., 2006). For instance, these bacteria were found in the Norwegian Sea on the cold methane seeps (Lein et al., 2000). It is interesting that during the expedition in 2014 aboard the Swedish scientific icebreaker “Oden” dissolved methane was found in low concentrations in the pore water of the surface sediments (D. Kosmach and V. Bruchert, personal communications), and also it was found in low concentrations even in the areas of powerful bubble jets (Shakhova et al., 2015), where the concentrations of the dissolved methane in the water column reached values 2–3 orders of magnitude higher than the corresponding equilibrium values (with respect to the atmosphere) of the concentrations. The authors believe that such a “paradoxical” situation is explained by the fact that diffusion methane is almost completely withdrawn from treatment on the sulfate-reduction biofilter, but the massive release of bubble methane (with the average bubble radius of 0.7 cm (Shakhova et al., 2015)) occurs in the mega-seep areas by the through discharge channels — gas outlets, as suggested in the earlier works (Shakhova et al., 2009a,b; 2010b). To get a more accurate answer, additional complex biogeochemical, geophysical, and geological studies are required (with sampling of the core of the sediments up to 5–6 m long), which are planned by the authors team for 2020–2021.

**Principal Component Analysis (PCA).** The data obtained were subjected to PCA by the four main components (Pomerantsev, 2014). The analysis showed the separation of the studied samples in the space PC1–PC2 into two classes: Class 1 and Class 2 (Fig. 13a, b). The Class 1 samples are characterized by high sulfur content on average (and also

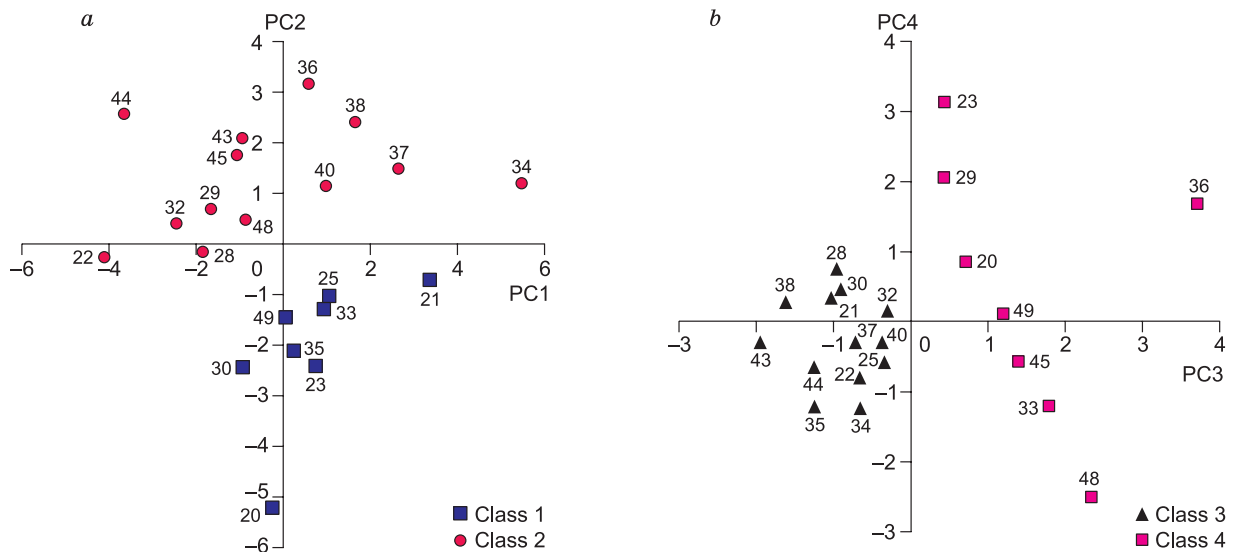


**Fig. 13.** The diagrams of the space of the main components PC1 – PC2 (a) and PC3 – PC4 (b). The numbers indicate sampling stations.

have higher HI index on average and lower average Pr/Phy ratio), i.e. they are characterized by a more reducing sedimentation environment compared to the Class 2 samples. All samples that are in the methane emission zones fall into this group, except for the sample collected at station 21. Somewhat apart is station 20. The sample of this station is characterized by a high content of polyaromatic hydrocarbons, as well as a maximum CPI index. In the space PC3 — PC4 (Fig. 13b), the separation almost corresponds to the principle of dividing the samples into two classes in accordance with stations location: Class 3 (zones of methane emissions) and Class 4 (outside the zones of methane emissions). All samples located in the methane emission zones belong to the Class 3 group. However, it is worth noting that the division is incomplete, since the samples of stations 25, 30 and 35 also fall into the Class 3 group and station 36 is located somewhat separately. This indicates that within the study area there are other factors as yet known, which require additional research.

## CONCLUSIONS

1) The triterpenoids found in the sediment composition, which are the constituent links of the diagenetic transformation chain of organic matter of bacterial origin in the methane emission areas, indicate that methane has been emitted for a long time (Talbot et al., 2014, 2016; Volkman et al., 2015). In places where methane is released, an intensive activity of a consortium of methanotrophs and sulfate reducers takes place.

2) A positive correlation was found between the content of some biomarkers relative to the pelite fraction and the total organic carbon content at the stations with the recorded intense methane bubbling. For instance, the average content of the  $C_{30}$  hopenes at the methane stations is twice as high as that at the background ones, while the average concentration of  $C_{32}$   $\alpha\beta$ -hopanes at the methane seep areas is 1.5-fold higher. It is also likely that due to the inflow of the OM of the petroleum origin, we observe an increase in the content of  $C_{30}$   $\alpha\beta$ -hopane (1.5-fold higher on average at the “seepage” stations) and the decrease in the value of the moretane index relative to the hopane ( $C_{31}$ ) index.

3) The detection of biphenyl mainly at the stations enriched with marine organic matter, as well as the detection of  $\alpha\beta$ - $C_{32}$  hopanes, Ts traces, the reduced CPI value for samples of one of the methane stations (№ 44) and lower values of the moretane index suggest the migration of the petroleum hydrocarbons (micro-oil) through gas outlet channels from the underlying horizons, through the thawed subsea permafrost; however, this hypothesis requires additional research.

4) On average, the OC content in the areas of jet emission of methane is lower compared to the stations located outside the methane emission zones, which may be connected with diluting action due to the filling of the sediments with sand

from the deeper horizons and partial removal of the fine pelite fraction.

5) Alkylbenzenes identified in the sediments are predominantly phenylalkanes and have a marine genesis. Squalene is primarily of terrigenous origin, however, part of it is produced under marine conditions by methanotrophic microorganisms in the zones of methane emissions. Polyaromatic hydrocarbons—phenanthrene and its alkyl substituted homologues, pyrene have one source of formation with phenylalkanes, most likely originating from marine biota, and biphenyl has another — yet insufficiently studied source.

6) The composition of the organic matter of the sediments in the eastern part of the polygon is dominated by more diagenetically transformed material of terrigenous origin, which is probably due to the transport of erosional OC from Kotel'nyi Island, where thermoerosion banks are widespread.

This work was supported by the Russian Science Foundation (project № 15-17-20032, headed by N.E. Shakhova) in the International Research Laboratory for Arctic Seas Carbon of the National Research Tomsk Polytechnic University and in the Arctic Research Laboratory of the V.I. Il'ichev Pacific Oceanological Institute of the Far Eastern Branch of the Russian Academy of Sciences (Megagrant of the Russian Government, contract #14.Z50.31.0012). E.V. Gershelis is also grateful to the Russian Foundation for Basic Research (project № 18-35-00572 mol-a). The research is funded from Tomsk Polytechnic University Competitiveness Enhancement Program grant, Project Number #CEP-SESE-299/2019.

## REFERENCES

- Ageta, H., Shiojima, K., Arai, Y., Suzuki, H., Kiyotani, T., 1994. NMR-spectra of triterpenoids. 2. Hopenes and migrated hopenes. *Chem. Pharm. Bull.* 42, 39–44.
- Aloisi, G., Bouloubassi, N.V., Heijs, S.K., Pancost, R.D., Pierre, C., Damste, J.S.S., Gottschal, J.C., Forney, L.J., Rouchy J.M., 2002.  $CH_4$ -consuming microorganisms and the formation of carbonate crusts at cold seeps. *Earth Planet. Sci. Lett.* 203 (1), 195–203.
- Anderson, L.G., Björk G., Jutterström S., Pipko I., Shakhova N. Semiletov I., Wählström, I., 2011. East Siberian Sea, an Arctic region of very high biogeochemical activity. *Biogeosciences* 8, 1745–1754.
- Andieva, T.A., 2008. Tectonic position and main structures of the Laptev Sea. *Neftegazovaya Geologiya. Teoriya i Praktika* 3 (1), [http://www.ngtp.ru/rub/4/8\\_2008.pdf](http://www.ngtp.ru/rub/4/8_2008.pdf).
- Belenitskaya, G.A., 2002. Fluid sedimentogenesis – modern scientific direction of sedimentary geology: state, objects, tasks, in: Leningrad school of lithology. Materials of the All-Russian Lithological Conference dedicated to the 100<sup>th</sup> anniversary of L.B. Rukhin, 2012., St. Petersburg. Vol. 1, pp. 30–32.
- Blumenberg, M., Mollenhauer, G., Zabel, M., Reimer, A., Thiel, V., 2010. Decoupling of bio- and geohopanooids in sediments of the Benguela Upwelling System (BUS). *Org. Geochem.* 41, 1119–1129.
- Brassell, S.C., Farrimond, P., 1986. Fluctuations in biological marker composition within a Cenomanian black shale from the Angola Basin. *Mitt. Geol. Palaeontol. Inst. Univ. Hamburg* 60, 311–338.
- Bröder, L., Tesi, T., Andersson, A., Eglinton, T.I., Semiletov, P.I., Dudarev, O.V., Roos, P., Gustafsson, Ö., 2016a. Historical records

- of organic matter supply and degradation status in the East Siberian Sea. *Org. Geochem.* 91, 16–30.
- Bröder, L., Tesi, T., Salvado, J.A., Semiletov, I.P., Dudarev, O.V., Gustafsson, Ö., 2016b. Fate of terrigenous organic matter across the Laptev Sea from the mouth of the Lena River to the deep sea of the Arctic interior. *Biogeosciences* 13, 5003–5019.
- Charkin, A.N., Dudarev, O.V., Semiletov, I.P., Kruhmalev, A.V., Vonk, J.E., Sánchez-García, L., Karlsson, E., Gustafsson, Ö., 2011. Seasonal and interannual variability of sedimentation and organic matter distribution in the Buor Khaya Gulf – the primary recipient of input from Lena River and coastal erosion in the SE Laptev Sea. *Biogeosciences* 8, 2581–2594.
- Cooke, M.P., van Dongen, B., Talbot, H., Semiletov, I.P., Shakhova, N., Guo, L., Gustafsson, Ö., 2009. Bacteriohopanepolyol biomarker composition of organic matter exported to the Arctic Ocean by seven of the major Arctic rivers. *Org. Geochem.* 40 (11), 1151–1159.
- Damste, J.S.S., Rijpstra, W.I.C., Schouten, S., Fuerst, J.A., Jetten, M.S.M., Strous, M., 2004. The occurrence of hopanoids in planctomycetes: Implications for the sedimentary biomarker record. *Org. Geochem.* 35(5), 561–566.
- Damste, J.S.S., Shouten, S., Volkman, J.K., 2014. C<sub>27</sub>–C<sub>30</sub> neohop-13(18)-enes and their saturated and aromatic derivatives in sediments: Indicators for diagenesis and water column stratification. *Geochim. Cosmochim. Acta* 133, 402–421.
- Damste, J.S.S., van Duin, A.C.T., Hollander, D., Kohlen, M.E.L., de Leeuw, J.W., 1995. Early diagenesis of bacteriohopanepolyol derivatives: Formation of fossil homohopaneoids. *Geochim. Cosmochim. Acta* 59 (4), 5141–5147.
- de Angelis, M.A., Reysenback, A.-L., Baross, J.A., 1991. Surfaces of hydrothermal vent invertebrates: sites of elevated microbial methane oxidation activity. *Limnol. Oceanogr.* 36, 570–577.
- Dobrovolsky, A.D., Zalogin, B.S., 1982. *The USSR Seas* [in Russian]. Moscow University Press, Moscow.
- Donk, E.N., 2015. Bacteria Do It Differently: An Alternative Path to Squalene. *ACS Cen. Sci.* 1 (2), 64–65.
- Drachev, S.S., 2000. Tectonics of the Rift System of the Laptev Sea bottom. *Geotectonics* 6, 43–58.
- Drenzek, N.J., Montlucon, D.B., Yunker, M.B., Macdonald, R.W., Eglinton, T.I., 2007. Constraints on the origin of sedimentary organic carbon in the Beaufort Sea from coupled molecular <sup>13</sup>C and <sup>14</sup>C measurements. *Mar. Chem.* 103, 146–162.
- Dudarev, O.V., Charkin, A.N., Shakhova, N.E., Mazurov, A.K., Semiletov, I.P., 2016. Modern Lipomorphogenesis on the Russia Eastern Arctic Shelf [in Russian]. TPU, Tomsk.
- Dworkin, M., Falkow, S., Rosenberg, E., Schleifer, K.-H., Stackebrandt, E., 2006. *The Prokaryotes: A Handbook on the Biology of Bacteria*. Vol. 2: Ecophysiology and biochemistry, Springer-Verlag, New York.
- Eganhouse, R.P., 1986. Long-chain alkylbenzenes: Their analytical chemistry, environmental occurrence and fate. *Int. J. Environ. Anal. Chem.* 26, 241–263.
- Eglinton, G., Gonzalez, A.G., Hamilton, R.J., Raphael, R.A., 1962. Hydrocarbon constituents of the wax coatings of plant leaves—a taxonomic survey. *Phytochemistry* 1, 89–102.
- Ellis, L., Langworthy, T.A., Winans, R.E., 1996. Occurrence of phenylalkanes in some Australian crude oils and sediments. *Org. Geochem.* 24 (1), 57–69.
- Fahl, K., Stein, R., 1997. Modern organic carbon deposition in the Laptev Sea and the adjacent continental slope: surface water productivity vs terrigenous input. *Org. Geochem.* 26 (5/6), 379–390.
- Feng, X., Gustafsson, O., Holmes, R.M., Vonk, J.E., van Dongen, B.E., Semiletov, I.P., Dudarev, O.V., Yunker, M.B., Macdonald, R.W., Montlucon, D.B., Eglinton, T.I., 2015. Multi-molecular tracers of terrestrial carbon transfer across the pan-Arctic: comparison of hydrolysable components with plant wax lipids and lignin phenols. *Biogeosciences* 12, 4841–4860.
- Fischer, W.W., Summons, R.E., Pearson, A., 2005. Targeted genomic detection of biosynthetic pathways: anaerobic production of hopanoid biomarkers by a common sedimentary microbe. *Geobiology* 3, 33–40.
- Franke, D., Hinz, K., Oncken, O., 2001. The Laptev Sea Rift. *Mar. Petrol. Geol.* 18 (10), 1083–1127.
- Galimov, E.M., Kodina, L.A., 1982. Investigation of organic matter and gases in sedimentary strata of the World Ocean bottom [in Russian]. Nauka, Moscow.
- Goncharov, I.V., 1987. Geochemistry of oils in Western Siberia [in Russian]. Nedra, Moscow.
- Gramberg, I.S., Kulakov, Yu.N., Pogrebitsky, Yu.E., Sorokov, D.S., 1983. Arctic oil and gas super basin, in: *Proceed. of 11th World Petroleum Congress*. London, pp. 93–99.
- Grigoriev, M.N., Vasiliev, A.A., Rachold, V., 2004. Siberian Arctic coasts: sediment and organic carbon fluxes in connection with permafrost degradation, in: *AGU Fall Meeting*. San Francisco, p. 85.
- Grosjean, E., Logan, A.G., 2007. Incorporation of organic contaminants into geochemical samples and an assessment of potential sources: Examples from Geoscience Australia marine survey S282. *Org. Geochem.* 38 (6), 853–869.
- Gustafsson, Ö., van Dongen, B.E., Vonk, J.E., Dudarev, O.V., Semiletov, I.P., 2011. Widespread release of old carbon across the Siberian Arctic echoed by its large rivers. *Biogeosciences* 8, 1737–1743.
- Han, J., Calvin, M., 1969. Hydrocarbon distribution of algae and bacteria, and microbiological activity in sediments. *Proc. Natl. Acad. Sci. USA.* 64 (2), 436–443.
- Hanson, R.S., Hanson, T.E., 1996. Methanotrophic bacteria. *Microbiol. Rev.* 60 (2), 439–471.
- Hartner, T., Straub, K.L., Kannenberg, E., 2005. Occurrence of hopanoid lipids in anaerobic *Geobacter* species. *FEMS Microbiol. Lett.*, 243, 59–64.
- Hedges, J.I., Prahl, F.G., 1993. Early diagenesis: Consequences for applications of molecular biomarkers. *Org. Geochem. Principles Appl.* 237–253.
- Helmke, E., Jürgens, J., Tausendfreund, M., Wollenburg, J., Shank, T., Edmundson, H., Humphris, S., Nakamura, K., Liliebladh, B., Windsor, P., Singh H., Reves-Sohn, R., 2007. Microbial communities at non-volcanic and volcanic sites of the Gakkel Ridge, in: *AGU Fall Meeting*, San Francisco, December 2007.
- Imaev, V.S., Imaeva, L.P., Kozmin, B.M., 1990. Active rifts and seismotectonics of Northeastern Yakutia [in Russian]. YaSC SB AS USSR, Yakutsk.
- Jakobsson, M., Macnab, R., Mayer, L., Anderson, R., Edwards, M., Hatzky, J., Schenke, H. W., Johnson, P., 2008. An improved bathymetric portrayal of the Arctic Ocean: Implications for ocean modeling and geological, geophysical and oceanographic analyses. *Geoph. Res. Lett.* 35 (7), L07602.
- Joye, S.B., Boetius, A., Orcutt, N.B., Montoya, J.P., Schulz, H.N., Erickson, M.J., Lugo, S.K., 2004. The anaerobic oxidation of methane and sulfate reduction in sediments from Gulf of Mexico cold seeps. *Chem. Geol.* 205, 219–238.
- Karlsson, E.S., Charkin, A., Dudarev, O., Semiletov, I., Vonk, J.E., Sánchez-García, L.S., Andersson, A., Gustafsson, O., 2011. Carbon isotopes and lipid biomarker investigation of sources, transport and degradation of terrestrial organic matter in the Buor-Khaya Bay, SE Laptev Sea. *Biogeosciences* 8, 1865–1879.
- Kashirtsev, V.A., Mikulenko, K.I., Safronov, A.F., Zueva, I.N., Chalaya, O.N., 2004. Geochemistry of the Vendian–Cambrian oil manifestations of the Lena–Amginsky interfluvium (Siberian platform), in: *Topical Issues of Oil and Gas Geology of the Siberian Platform* [in Russian]. Yakutsk, pp. 156–168.
- Kashirtsev, V.A., 2003. Organic Geochemistry of Naphthides of the East Siberian Platform [in Russian]. YaB SB RAS Publ., Yakutsk.
- Kashirtsev, V.A., Kim, N.S., Fursenko, E.A., Dzyuba, O.S., Fomin, A.N., Chalaya, O.N., 2013. Genesis of oils and oil shows of the

- Anabar-Khatanga Saddle (Arctic Sector of the Siberian Platform). *Geologiya i mineral'no-syr'evye resursy Sibiri* 1, 54–63.
- Kasymkaya, M.V., Tipenko, G.S., 2005. Simulation of taliks evolution on the Laptev sea Shelf during the Last Transgression, in: 2nd European conference on permafrost EUCOPII, 12–16 June 2005, Potsdam, Germany, pp. 162–163.
- Knittel, K., Boetius, A., 2009. Anaerobic oxidation of methane: progress with an unknown process. *Microbiology* 63, 311–334.
- Kontorovich, V.A., Kontorovich, A.E., Gubin, I.A., Zoteev, A.M., Lapkovsky, V.V., Malyshev, N.A., Soloviev, M.V., Fradkin, G.S., 2013. The Neoproterozoic-Phanerozoic section of the Anabar-Lena province: structural framework, geological model, and petroleum potential. *Russian Geology and Geophysics (Geologiya i Geofizika)* 54 (8), 980–996 (1253–1274).
- Kristjansson, J.K., Schönheit, P., Thauer, R.K., 1982. Different  $K_s$  values for hydrogen of methanogenic bacteria and sulfate-reducing bacteria: an explanation for the apparent inhibition of methanogenesis by sulfate. *Archives of Microbiology* 131 (3), 278–282.
- Ladygina, N.A., Dedyukhina, E.G., Vainshtein, M.B., 2006. Review on microbial synthesis of hydrocarbons. *Process Biochem.* 41 (5), 1001–1014.
- Leifer, I., Chernykh, D., Shakhova, N., Semiletov, I., 2017. Sonar gas flux estimation by bubble insonification: application to methane bubble fluxes from the East Siberian Arctic Shelf Seabed. *The Cryosphere* 11, 1333–1350.
- Lein, A.Yu., Ivanov, M.V., 2009. Biogeochemical Cycle of Methane in the Ocean [in Russian]. Nauka, Moscow.
- Lein, A.Yu., Pimenov, N.V., Savvichev, A.S., Pavlova, G.A., Vogt, P., Bogdanov, Yu.A., Sagalevich, A.M., Ivanov, M.V., 2000. Methane as a source of organic matter and carbon dioxide of carbonates at a cold seep in the Norway Sea. *Geochemistry international* 38 (3), 232–245.
- Lein, A.Yu., Rusanov, I.I., Pimenov, N.V., Savvichev, A.S., Miller, Yu.M., Pavlova, G.A., Ivanov, M.V., 1996. Biogeochemical processes of the Sulphur and Carbon Cycles in the Kara Sea. *Geochemistry international* 34 (11), 925–941.
- Lengeler, J.W., Drews, G., Schlegel, H.G. (Eds.), 1999. *Biology of the Prokaryotes*. Stuttgart, Thieme, New-York.
- Leonov, M.G., Baluev, A.S., Kuzmichev, A.B., Leonov, Yu.G., Mazarovich, A.O., Polyakova, I.D., Sokolov, S.D., Sokolov, S.Yu., Khain, V.E., Khutorsky, M.D., 2007. Tectonics of the Russia Arctic Shelf in studies of the Geological Institute of the Russian Academy of Sciences, in: *Arctic Oil and Gas. Materials of the International Scientific and Technical Conference* [in Russian]. Interkontakt Nauka, Moscow, pp. 12–34.
- Luchin, V.A., Semiletov, I.P., Weller, G.E., 2002. Changes in the Bering Sea region: atmosphere – ice – water system in the second half of the twentieth century. *Progress Oceanogr.* 55 (1–2), 23–44.
- Macdonald, R.W., Anderson, L.G., Christensen, J.P., Miller, L.A., Semiletov, I.P., Stein, R., 2008. The Arctic Ocean: budgets and fluxes, in: Liu, K.-K., Atkinson, L., Quinones, R., Talaue-McManus, L. (Eds.). *Carbon and Nutrient Fluxes in Continental Margins: A Global Synthesis*. Springer-Verlag, pp. 291–303.
- Malyshev, N.A., Obmetko, V.V., Borodulin, A.A., 2010. Assessment of the prospect of oil and gas potential of sedimentary basins of the Eastern Arctic. *Nauchno-tekhnicheskii vestnik Rosneft'* 1, 20–28.
- Matsueda, H., Handa, N., Inoue, I., Takano, H., 1986. Ecological significance of salp fecal pellets collected by sediment traps in the eastern North Pacific. *Mar. Biol.* 91, 421–31.
- Matsumoto, G.I., Watanuki, K., 1990. Geochemical features of hydrocarbon and fatty acid in sediments of the inland hydrothermal environments of Japan. *Org. Geochem.* 15 (2), 199–208.
- Medeiros, P.M., Simoneit, B.R.T., 2007. Gas chromatography coupled to mass spectrometry for analyses of organic compounds and biomarkers as tracers for geological, environmental, and forensic research. *J. Separat. Sci.* 30, 1516–1536.
- Melenevskii, V.N., Saraev, S.V., Kostyreva, E.A., Kashirtsev, V.A., 2017. Diagenetic transformation of organic matter of the Holocene Black Sea sediments according to pyrolysis data. *Russian Geology and Geophysics (Geologiya i Geofizika)* 58 (2), 225–239 (273–289).
- Michaelis, W., Seifert, R., Nauhaus, K., Treude, T., Thiel, V., Blumenberg, M., Knittel, K., Gieseke, A., Peterknecht, K., Pape, T., Boetius, A., Amann, R., Jorgenson, B.B., Widdel, F., Peckmann, J., Pimenov, N., Gulin, M.B., 2002. Microbial reefs in the black sea fueled by anaerobic methane oxidation. *Science* 297, 1013–1015.
- Moldowan, J.M., Fago, F.J., Carlson, R.M.K., Young, D.C., Van Duyne G., Clardy J., Schoell M., Pillinger C.T., Watt D.S., 1991. Rearranged hopanes in sediments and petroleum. *Geochim. Cosmochim. Acta* 55, 3333–3353.
- Nicolosky, D., Shakhova, N., 2010. Modeling sub-sea permafrost in the East-Siberian Arctic Shelf: the Dmitry Laptev Strait. *Environ. Res. Lett.* 5 (1), 015006.
- Nicolosky, D.J., Romanovsky, V.E., Romanovskii, N.N., Kholodov, A.L., Shakhova, N.E., Semiletov, I.P., 2012. Modeling sub-sea permafrost in the East Siberian Arctic Shelf: The Laptev Sea region. *J. Geoph. Res.* 117, F03028.
- Oremland, R.S., Culbertson, C.W., 1992. Importance of methane-oxidizing bacteria in the methane budget as revealed by the use of a specific inhibitor. *Nature* 356, 421–423.
- Osborne, K.A., Gray, N.D., Sherry, A., Leary, P., Mejeha, O., Bischoff, J., Rush, D., Sidgwick, F.R., Birgel, D., Kalyuzhnaya, M.G., Talbot, H.M., 2017. Methanotroph-derived bacteriohopanepolyol signatures as a function of temperature related growth, survival, cell death and preservation in the geological record. *Environ. Microbiol. Rep.* 9(5), 492–500.
- Overduin, P.P., Hubberten, H.-W., Rachold, V., Romanovskii, N., Grigoriev, M.N., Kasymkaya, M., 2007. Evolution and degradation of coastal and offshore permafrost in the Laptev and East Siberian Seas during the last climatic cycle. *Coastal changes: Interrelation of climate and geological processes. Geol. Soc. Amer., Spec. Pap.* 426, 97–111.
- Panova, E.V., Ruban, A.S., Dudarev, O.V., Tesi, T., Bröder, L., Gustafsson, Ö., Grinko, A.A., Shakhova, N.E., Goncharov, I.V., Mazurov, A.K., Semiletov, I.P., 2017. Lithological features of surface sediment and their influence on organic matter distribution across the East-Siberian Arctic Shelf. *Bulletin of the TPU. Geo Assets Engineering* 328 (8), 94–105.
- Peckmann, J., Thiel, V., Michaelis, W., Clari, P., Gaillard, C., Martire, L., Reitner, J., 1999. Cold seep deposits of Beauvoisin (Oxfordian; southeastern France) and Marmorito (Miocene; northern Italy): microbially induced authigenic carbonates. *Int. J. Earth Sci.* 88, 60–75.
- Petelin, V.P., 1961. New method of water mechanical analysis of marine bottom sediments. *Okeanologiya* 1 (1), 143–148.
- Peters, K.E., Walters, C.C., Moldowan, J.M., 2005. *The Biomarker Guide, Part I, Biomarkers and Isotopes in the Environmental and Human History and Part II Biomarkers and Isotopes in Petroleum Exploration and Earth History*. Cambridge University Press, Cambridge.
- Petrov, A.A., 1987. *Petroleum Hydrocarbons*, Springer-Verlag, Berlin Heidelberg.
- Petrova, V.I., Batova, G.I., Kursheva, A.V., Litvinenko, I.V., 2010. Geochemistry of organic matter of bottom sediments in the rises of the central Arctic Ocean. *Russian Geology and Geophysics (Geologiya i Geofizika)* 51 (1), 88–97 (113–125).
- Petrova, V.I., Batova, G.I., Kursheva, A.V., Litvinenko, I.V., Savinov, V.M., Savinova, T.N., 2008. Geochemistry of polycyclic aromatic hydrocarbons in the bottom sediments of the Eastern Arctic shelf. *Oceanology* 48 (2), 196–203.
- Pipko, I.I., Pugach, S.P., Semiletov, I.P., Anderson, L.G., Shakhova, N.E., Gustafsson, Ö., Repina, I.A., Spivak, E.A., Charkin, A.N.,

- Salyuk, A.N., Shcherbakova, K.P., Panova, E.V., Dudarev, O.V., 2017. The dynamics of the carbon dioxide system in the outer shelf and slope of the Eurasian Arctic Ocean. *Ocean Sci.* 13, 997–1016.
- Pipko, I.I., Semiletov, I.P., Pugach, S.P., Wählström, I., Anderson, L.G., 2011. Interannual variability of air-sea CO<sub>2</sub> fluxes and carbon system in the East Siberian Sea. *Biogeosciences* 8, 1987–2007.
- Pomerantsev, A.L., 2014. *Chemometrics in Excel*. Wiley.
- Prahl, F.G., Hayes, J., Xie T.-M., 1992. Diploptene: an indicator of terrigenous organic carbon in Washington coastal sediments. *Limnol. and Oceanogr.* 37 (6), 1290–1299.
- Proshutinsky, A., Timmermans, M.-L., Ashik, I., Beszczynska-Moeller, A., Carmack, E., Frolov, I., Ingvaldsen, R., Itoh, M., Kikuchi, T., Krishfield, R., McLaughlin, F., Loeng, H., Nishino, S., Puickart, R., Rabe, B., Rudels, B., Semiletov, I., Schauer, U., Shakhova, N., Shimada, K., Sokolov, V., Steele, M., Toole, J., Weingartner, T., Williams, W., Woodgate, R., Yamamoto-Kawai, M., Zimmermann, S., 2012. The Arctic Ocean. *State of the Climate in 2011*. *Bull. Amer. Meteorol. Soc.* 93 (7), S142–S145.
- Pugach, S.P., Pipko, I.I., Semiletov, I.P., Sergienko, V.I., 2015. Optical characteristics of the colored dissolved organic matter on the East Siberian shelf. *Dokl. Earth Sci.* 465 (2), 1293–1296.
- Pugach, S.P., Pipko, I.I., Shakhova, N.E., Shirshin, E.A., Perminova, I.V., Gustafsson, Ö., Bondur, V.G., Ruban, A.S., Semiletov, I.P., 2018. DOM and its optical characteristics in the Laptev and East Siberian seas: Spatial distribution and inter-annual variability (2003–2011). *Ocean Sci.* 14, 87–103.
- Rachold, V., Alabyan, A., Hubberten, H.-W., Korotaev, V.N., Zaitsev, A.A., 1996. Sediment transport to the Laptev Sea—hydrology and geochemistry of the Lena River. *Polar Res.* 15 (2), 183–96.
- Report of the Intergovernmental Panel on Climate Change, 2007. URL: [http://www.ipcc.ch/pdf/assessment-report/ar4/syr/ar4\\_syr\\_ru.pdf](http://www.ipcc.ch/pdf/assessment-report/ar4/syr/ar4_syr_ru.pdf) [circulation date 02.04.2013].
- Rieley, G., Collier, R.J., Jones, D.M., Eglinton G., 1991. Biogeochemistry of Ellesmere Lake, U.K.: I. Source correlation of leaf wax inputs to the sedimentary lipid record. *Org. Geochem.* 17 (6), 901–912.
- Rohmer, M., Bouvier-Nave, P., Ourisson, G., 1984. Distribution of hopanoid triterpenes in prokaryotes. *J. Gen. Microbiol.* 130, 1137–1150.
- Romankevich, E.A., Lisitsyn, A.P., Vinogradov, M.E. (Eds.), 2003. *The Pechora Sea: integrated research [in Russian]*. More, Moscow.
- Romankevich, E.A., Vetrov, A.A., 2001. *Carbon Cycle in the Russian Arctic Seas [in Russian]*. Nauka, Moscow.
- Ruff, S.E., Arnds, J., Knittel, K., Amann, R., Wegener, G., Ramette, A., Boetius, A., 2013. Microbial communities of deep-sea methane seeps at Hikurangi continental margin (New Zealand). *PLoS One*, Sep 30; 8 (9), doi.org/10.1371/journal.pone.0072627.
- Rush, D., Osborne, K.A., Birgel, D., Kappler, A., Hirayama, H., Peckmann, J., Poulton, S.W., Nickel, J.C., Mangelsdorf, K., Kalyuzhnaya, M., Sidgwick, F.R., Talbot, H.M., 2016. The bacteriohopanepolyol inventory of novel aerobic methane oxidizing bacteria reveals new biomarker signatures of aerobic methanotrophy in marine systems. *PloS One*, Nov. 8;11 (11), doi.org/10.1371/journal.pone.0165635.
- Safronov, A.F., Sivtsev, A.I., Chalaya, O.N., Zueva, I.N., Sokolov, A.N., Fradkin, G.S., 2013. Initial geologic hydrocarbon resources of the Laptev Sea shelf. *Russian Geology and Geophysics (Geologiya i Geofizika)* 54 (8), 997–1000 (1275–1279).
- Salvado, J.A., Tesi, T., Sundbom, M., Karlsson, E., Krusa, M., Semiletov, I.P., Panova, E., Gustafsson, Ö., 2016. Contrasting composition of terrigenous organic matter in the dissolved, particulate and sedimentary organic carbon pools on the outer East Siberian Arctic Shelf. *Biogeosciences* 13, 6121–6138.
- Sánchez-García L., Alling V., Pugach S., Vonk J., van Dongen B., Humborg C., Dudarev O., Semiletov I., Gustafsson Ö., 2011. Inventories and behavior of particular organic carbon in the Laptev and East Siberian seas. *Global Biogeochem. Cycles* 25 (2), GB2007.
- Sapart, C.J., Shakhova, N., Semiletov, I., Jansen, J., Szidat, S., Kosmach, D., Dudarev, O., van der Veen, C., Egger, M., Sergienko, V., Salyuk, A., Tumskey, V., Tison, J.L., Rockmann, T., 2017. The origin of methane in the East Siberian Arctic Shelf unraveled with triple isotope analysis. *Biogeosciences* 14, 2283–2292.
- Savelieva, N.I., Semiletov, I.P., Vasilevskaya, L.N., Pugach, S.P., 2000. A climate shift in seasonal values of meteorological and hydrological parameters for Northeastern Asia. *Prog. Oceanogr.* 47, (2–4), 279–297.
- Savvichev, A.S., Zakharova, E.E., Veslopolova, E.F., Rusanov, I.I., Lein, A.Yu., Ivanov, M.V., 2010. Microbial processes of the carbon and sulfur cycles in the Kara Sea. *Oceanology* 50 (6), 893–908.
- Selver, A.D., Sparkes, R.B., Bischoff, J., Talbot, H.M., Gustafsson, Ö., Semiletov, I.P., Dudarev, O.V., Boulton, S., van Dongen, B.E., 2015. Distributions of bacterial and archaeal membrane lipids in surface sediments reflect differences in input and loss of terrestrial organic carbon along a cross-shelf Arctic transect. *Org. Geochem.* 83–84, 16–26.
- Semiletov, I., Pipko, I., Gustafsson, Ö., Anderson, L.G., Sergienko, V., Pugach, S., Dudarev, O., Charkin, A., Gukov, A., Bröder, L., Andersson, A., Spivak, E., Shakhova, N., 2016. Acidification of East Siberian Arctic Shelf waters through addition of freshwater and terrestrial carbon. *Nat. Geosci.* 9, 361–365.
- Semiletov, I., Shakhova, N., Romanovsky, V., 2004. Methane Climate Forcing and Methane Observations in the Siberian Arctic Land-Shelf System. *World Resource Review* 16 (4), 503–541.
- Semiletov, I.P., Pipko, I.I., Pivovarov, N.Ya., Popov, V.V., Zimov, S.A., Voropaev, Yu.V., Daviodov, S.P., 1996. Atmospheric carbon emissions from northern lakes: a factor of global significance. *Atmos. Environ.* 30, 1657–1671.
- Semiletov, I.P., 1999. The failure of coastal frozen rock as an important factor in the biogeochemistry of the Arctic shelf water. *Dokl. Earth Sci.* 369, 1140–143.
- Semiletov, I.P., Dudarev, O.V., Pipko, I.I., Pugach, S.P., Sergienko, V.I., Chubik, P.S., Mazurov, A.K., Shakhova, N.E., 2017. The carbon cycle in the seas of the Eastern Arctic at the turn of the XX-th and XXI-st centuries. Book 1. *Transportation and Transformation of Carbon in the System “Land-Shelf” [in Russian]*. TPU: Tomsk.
- Semiletov, I.P., Pipko, I.I., Shakhova, N.E., Dudarev, O.V., Pugach, S.P., Charkin, A.N., McRoy, C.P., Kosmach, D., Gustafsson, Ö., 2011. Carbon transport by the Lena River from its headwaters to the Arctic Ocean, with emphasis on fluvial input of terrestrial particulate organic carbon vs. carbon transport by coastal erosion. *Biogeosciences* 8, 2407–2426.
- Semiletov, I.P., Savelieva, N.I., Weller, G.E., Pipko, I.I., Pugach, S.P., Gukov, A.Yu., Vasilevskaya, L.N., 2000. The Dispersion of Siberian River Flows into Coastal Waters: Meteorological, Hydrological and Hydrochemical Aspects, in: *The Freshwater Budget of the Arctic Ocean*. NATO Meeting/NATO ASI Series, E.L. Lewis (Ed.), Kluwer Academic Publishers, Dordrecht, pp. 323–367.
- Semiletov, I.P., Shakhova, N.E., Pipko, I.I., Pugach, S.P., Charkin, A.N., Dudarev, O.V., Kosmach, D.A., Nishino, S., 2013. Space–time dynamics of carbon stocks and environmental parameters related to carbon dioxide emissions in the Buor-Khaya Bay of the Laptev Sea. *Biogeosciences* 10, 5977–5996.
- Semiletov, I.P., Shakhova, N.E., Sergienko, V.I., Pipko, I.I., Dudarev, O., 2012. On Carbon transport and fate in the East Siberian Arctic Land-Shelf-Atmosphere System. *Environ. Res. Lett.* 7 (1), 015201.
- Sergienko, V.I., Lobkovskii, L.I., Semiletov, I.P., Dudarev, O.V., Dmitrievskii, N.N., Shakhova, N.E., Romanovskii, N.N., Kosmach, D.A., Nikol’skii, D.N., Nikiforov, S.L., Salomatin, A.S., Anan’ev, R.A., Roslyakov, A.G., Salyuk, A.G., Karnaukh, V.V., Chernykh, D.B., Tumskey, V.E., Yusupov, V.I., Kurilenko, A.V., Chuvilin, E.M., Bukhanov, B.A., 2012. The degradation of submarine permafrost and the destruction of hydrates on the shelf of east arctic seas as a potential cause of the “Methane Catastrophe”: some results of integrated studies in 2011. *Dokl. Earth Sci.* 446 (1), 1132–1137.

- Shakhova, N., Semiletov, I., Gustafsson, O., Sergienko, V., Lobkovsky, L., Dudarev, O., Tumskey, V., Grigoriev, M., Mazurov, A., Salyuk, A., Ananiev, R., Koshurnikov, A., Kosmach, D., Charkin, A., Dmitrevsky, N., Karnaukh, V., Gunar, A., Meluzov, A., Chernykh, D., 2017. Current rates and mechanisms of subsea permafrost degradation in the East Siberian Arctic Shelf. *Nat. Commun.* 8, doi: 10.1038/ncomms15872.
- Shakhova, N., Semiletov, I., Leifer, I., Rekant, P., Salyuk, A., Kosmach, D., 2010a. Geochemical and geophysical evidence of methane release from the inner East Siberian Shelf. *J. Geoph. Res.* 115, doi:10.1029/2009JC005602.
- Shakhova, N., Semiletov, I., Leifer, I., Sergienko, V., Salyuk, A., Kosmach, D., Chernykh, D., Stubbs, C., Nicolsky, D., Tumskey, V., Gustafsson, Ö., 2014. Ebullition and storm-induced methane release from the East Siberian Arctic Shelf. *Nat. Geosci.* 7, 64–70.
- Shakhova, N., Semiletov, I., Salyuk, A., Yusupov, V., Kosmach, D., Gustafsson, Ö., 2010b. Extensive Methane Venting to the Atmosphere from Sediments of the East Siberian Arctic Shelf. *Science* 327, 1246–1250.
- Shakhova, N., Semiletov, I., Sergienko, V., Lobkovsky, L., Yusupov, V., Salyuk, A., Salomatin, A.A., Chernykh, D., Kosmach, D., Panteleev, G., Nicolsky, D., Samarkin, V., Joye, S., Charkin, A., Dudarev, O., Meluzov, A., Gustafsson, Ö., 2015. The East Siberian Arctic Shelf: towards further assessment of permafrost-related methane fluxes and role of sea ice. *Philos. Trans. R. Soc. London, Ser. A.*, 373 (2052), 20140451.
- Shakhova, N.E., Semiletov, I.P., 2009. Methane hydrate feedbacks, in: Sommerkorn, M., Hassol, S.J. (Eds.). *Arctic Climate Feedbacks: Global Implications*, Published by WWF International Arctic Programme August, pp. 81–92.
- Shakhova, N.E., Nicolsky, D.Yu., Semiletov, I.P., 2009b. Current state of subsea permafrost on the East Siberian Shelf: Tests of modeling results based on field observations. *Dokl. Earth Sci.* 429A (9), 1518–1521.
- Shakhova, N.E., Sergienko, V.I., Semiletov, I.P., 2009a. The contribution of the East Siberian shelf to the modern methane cycle. *Herald of the RAS* 79 (3), 237–246.
- Shakhova, N.E., Alekseev, V.A., Semiletov, I.P., 2010c. Predicted methane emission on the East Siberian shelf. *Dokl. Earth Sci.* 430, 190–193.
- Shiojima, K., Arai, Y., Masuda, K., Takase, Y., Ageta, T., Ageta, H., 1992. Mass-spectra of pentacyclic triterpenoids. *Chem. Pharm. Bull.* 40 (7), 1683–1690.
- Silva, T.R., Lopes, S.R.T., Spörl, G., Knoppers, B.A., Azevedo, D., 2013. Evaluation of anthropogenic inputs of hydrocarbon in sediment cores from a tropical Brazilian estuarine system. *Microchem. J.* 109, 178–188.
- Simoneit, B.R.T., 2004. Biomarkers (molecular fossils) as a geochemical indicators of life. *Adv. Space Res.* 33, 1255–1261.
- Smith, F.A., Wing, S.L., Freeman, K.H., 2007. Magnitude of the carbon isotope excursion at the Paleocene–Eocene thermal maximum: the role of plant community change. *Earth Plan. Sci. Lett.* 262, 50–65.
- Stein, R., Rullkotter, J., Littke, R., Schaefer, R.G., Welte, D.R., 1988. Organofacies reconstruction and lipid geochemistry of sediments from the Galicia Margin, Northeast Atlantic (ODP Leg 103). *Proc. Ocean Drilling Proj. Sci. Res.*, 103, 567–585.
- Stroh, J.N., Panteleev, G., Kirillov, S., Makhotin, M., Shakhova, N., 2015. Sea-surface temperature and salinity product comparison against external in situ data in the Arctic Ocean. *J. Geoph. Res.: Oceans* 120, 7223–7236.
- Sun, Y.-Z., Puttmann, W., 2001. Oxidation of organic matter in the transition zone of the Zechstein Kupferschiefer from the Sangerhausen Basin, Germany. *Energy Fuels* 15, 817–829.
- Talbot, H.M., Handley, L., Spencer-Jones, C.L., Dinga, B.J., Scheffuß, E., Mann, P.J., Poulsen, J.R., Spencer, R.G.M., Wabakanghanzi, J.N., Wagner, T., 2014. Variability in aerobic methane oxidation over the past 1.2 Myrs recorded in microbial biomarker signatures from Congo fan sediments. *Geochim. Cosmochim. Acta* 133, 387–401.
- Talbot, H.M., McClymont, E.L., Inglis, G.N., Evershed, R.P., Pancost, R.D., 2016. Origin and preservation of bacteriohopanepolyol signatures in Sphagnum peat from Bissendorfer Moor (Germany). *Org. Geochem.* 97, 95–110.
- Talbot, H.M., Summons, R.E., Jahnke, L.L., Cockell, C.S., Rohmer, M., Farrimond, P., 2008. Cyanobacterial bacteriohopanepolyol signatures from cultures and natural environmental settings. *Org. Geochem.* 39, 232–263.
- Tesi, T., Semiletov, I., Dudarev, O., Andersson, A., Gustafsson, Ö., 2016. Matrix association effects on hydrodynamic sorting and degradation of terrestrial organic matter during cross-shelf transport in the Laptev and East Siberian shelf seas. *J. Geophys. Res. Biogeosci.* 121 (3), 731–52.
- Tesi, T., Semiletov, I., Hugelius, G., Dudarev, O., Kuhry, P., Gustafsson, Ö., 2014. Composition and fate of terrigenous organic matter along the Arctic land–ocean continuum in East Siberia: Insights from biomarkers and carbon isotopes. *Geochim. Cosmochim. Acta* 133, 235–256.
- Thiel, V., Peckmann, J., Richnow, H.H., Luth, U., Reitner, J., Michaelis, W., 2001. Molecular signals for anaerobic methane oxidation in Black Sea seep carbonates and a microbial mat. *Mar. Chem.* 73, 97–112.
- Thomas, D.N., Fogg, G.E., Convey, P., Fritsen, C.H., Gili, J.-M., Gradinger, R., Laybourn-Parry, J., Reid, K., Walton, D.W.H., 2008. *The Biology of Polar Regions*. Oxford University Press.
- Timmers, P.H.A., Suarez-Zuluaga, D.A., van Rossem, M., Diender, M., Stams, A.J.M., Plugge, C.M., 2016. Anaerobic oxidation of methane associated with sulfate reduction in a natural freshwater gas source. *The ISME Journal* 10, 1400–1412.
- Tissot, B.P., Welte, D.H., 1984. *Petroleum Formation and Occurrence*. Springer-Verlag, New York.
- van Dongen, B.E., Schouten, S., Damste, J.S.S., 2006a. Preservation of carbohydrates through sulfurization in a Jurassic euxinic shelf sea: examination of the Blackstone Band TOC-cycle in the Kimmeridge Clay Formation, UK. *Org. Geochem.* 37, 1052–1073.
- van Dongen, B.E., Semiletov, I.P., Weijers, J.W.H., Gustafsson, O., 2008. Contrasting lipid biomarker composition of terrestrial organic matter exported from across the Eurasian Arctic by the five Great Russian Arctic rivers. *Global Biogeochem. Cycles* 22, 1–14.
- van Dongen, B.E., Talbot, H.M., Schouten, S., Pearson, P.N., Pancost, R.D., 2006b. Well preserved Palaeogene and Cretaceous biomarkers from the Kilwa area, Tanzania. *Org. Geochem.* 37 (5), 539–557.
- Vetrov, A.A., Romankevich, E.A., 2004. *The Organic Carbon Cycle in the Russian Arctic Seas*. Springer, Berlin.
- Vinogradov, V.A., Goryachev, Yu.V., Suprunenko, O.I., 2013. The Laptev Sea as a possible springboard for the effective development of the oil and gas resources of the Russia Arctic shelf. *Burenije i neft* 2, 15–18.
- Volkman, J.K., Zhang, Z., Xie, X., Qin, J., Borjigin, T., 2015. Biomarker evidence for *Botryococcus* and a methane cycle in the Eocene Huadian oil shale, NE China. *Org. Geochem.* 78, 121–134.
- Vonk, J.E., Sánchez-García, L., van Dongen, B.E., Alling, V., Kosmach, D., Charkin, A., Semiletov, I.P., Dudarev, O.V., Shakhova, N., Roos, P., Eglinton, T.I., Andersson, A., Gustafsson, Ö., 2012. Activation of old carbon by erosion of coastal and subsea permafrost in Arctic Siberia. *Nature* 489 (7414), 137–140.
- Vonk, J.E., Semiletov, I.P., Dudarev, O.V., Eglinton, T.I., Andersson, A., Shakhova, N., Charkin, A., Heim, B., Gustafsson, O., 2014. Preferential burial of permafrost derived organic carbon in Siberian Arctic shelf waters. *J. Geoph. Res.: Oceans*, 119 (12), 8410–8421.

- Wenger, L.M., Davis, C.L., Isaksen, G.H., 2002. Multiple controls on petroleum biodegradation and impact on oil quality. *SPE Reservoir Eval. Eng.* 5, 375–383.
- Wagner, D., Lipski, A., Embacher, A., Gattinger, A., 2005. Methane fluxes in permafrost habitats on the Lena Delta: effects of microbial community structure and organic matter quality. *Environ. Microbiol.* 7 (10), 1582–1592.
- Wightman, F., Lighty, D.L., 1982. Identification of phenylacetic acid as a natural auxin in the shoots of higher plants. *Physiologia Plantarum* 55 (1), 17–24.
- Xiao, X., Fahl, K., Muller, J., Stein, R., 2015. Sea-ice distribution in the modern Arctic Ocean: Biomarker records from trans-Arctic Ocean surface sediments. *Geochim. Cosmochim. Acta* 155, 16–29.
- Yunker, M.B., Backus, S.M., Pannatier, E.G., Jeffries, D.S., Macdonald, R.W., 2002. Sources and significance of alkane and PAH hydrocarbons in Canadian Arctic rivers. *Estuarine Coastal Shelf Sci.* 55, 1–31.
- Yunker, M.B., Macdonald, R.W., Cretney, W.J., Fowler, B.R., McLaughlin, F.A., 1993. Alkane, terpene and polycyclic aromatic hydrocarbon geochemistry of the Mackenzie River and Mackenzie shelf: Riverine contributions to Beaufort Sea coastal sediment. *Geochim. Cosmochim. Acta* 57, 3041–3061.
- Yunker, M.B., Macdonald, R.W., Veltkamp, D.J., Cretney, W.J., 1995. Terrestrial and marine biomarkers in a seasonally ice-covered Arctic estuary: Integration of multivariate and biomarker approaches. *Mar. Chem.*, 49, 1–50.
- Zhu, C., Wagner, T., Talbot, H.M., Weijers, J.W.H., Pan, J.-M., Pancost, R.D., 2013. Mechanistic controls on diverse fates of terrestrial organic components in the East China Sea. *Geochim. Cosmochim. Acta* 117, 129–143.

*Editorial responsibility:* L.M. Burshtein